# NUCLEAR MAGNETIC RESONANCE APPLIED TO THE STUDY OF SINGLE CRYSTALS

Daniel Hyndman

A Thesis Submitted for the Degree of PhD
at the
University of St Andrews

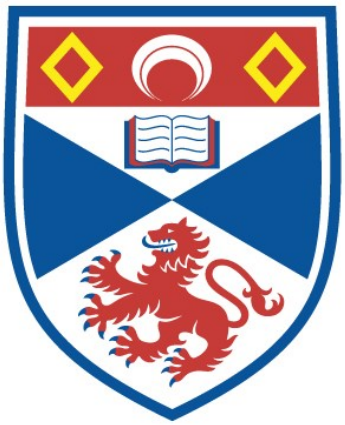

1955

# NUCLEAR MAGNETIC RESONANCE APPLIED TO THE STUDY OF SINGLE CRYSTALS

BEING

A THESIS PRESENTED BY

DANIEL HYNDMAN, B.Sc.

TO THE

UNIVERSITY OF ST. ANDREWS

IN APPLICATION FOR THE DEGREE

OF DOCTOR OF PHILOSOPHY.




ProQuest LLC.
789 East Eisenhower Parkway
P.O. Box 1346
Ann Arbor, MI 48106 – 1346

## DECLARATION

I hereby declare that the following Thesis is based on the results of experiments carried out by me, that the Thesis is my own composition, and that it has not previously been presented for a Higher Degree.

The research was carried out in the Physical Laboratory of St. Salvator's College of the University of St. Andrews under the direction of Dr. E.R.Andrew (now Prof. E.R.Andrew, University College of North Wales) from 1952 to 1954 and under the direction of Dr. F.A.Rushworth from 1954 to 1955.

## CERTIFICATE

I certify that Daniel Hyndman, B.Sc., has spent nine terms at research work in the Physical Laboratory of St. Salvator's College of the University of St. Andrews, that he has fulfilled the conditions of Ordinance No. 16 (St. Andrews) and that he is qualified to submit the accompanying Thesis in application for the Degree of Doctor of Philosophy.

Director of Research

## CAREER

I matriculated in the University of St. Andrews in October 1948 and followed a course in Mathematics and Natural Philosophy which led to my graduating in July 1952 with the degree of Bachelor of Science (First Class Honours in Natural Philosophy).

Having been awarded a University Post-Graduate Research Scholarship, I commenced research in August 1952 on the work which is now being submitted as a Ph.D. Thesis.

CONTENTS

CONTENTS (Cont'd)

# 1. INTRODUCTION.

## Nuclear Magnetic Resonance applied to the Study of Single Crystals.

Since its discovery in 1946 over 400 papers have been published on nuclear magnetic resonance of which more than 50% are related to problems in the structure of matter. This fact illustrates the scope of this comparatively new technique in the field of structural investigations. In addition nuclear magnetic resonance can give information concerning molecular motion in the solid state.

The work reported in this thesis is concerned with this field of research. An account is given of the application of nuclear magnetic resonance to the study of single crystals of Urea and Rochelle Salt.

## SECTION 2.

## 2. THEORY.

### 2.1. General.

Nuclear magnetic resonance has several features in common with the celebrated experiments of Rabi and his co-workers on atomic and molecular beams. Both techniques require a large steady magnetic field with a small rotating magnetic field polarised at right angles to the large field. In addition, the detection of the reorientation of magnetic nuclei in the applied field is effected in each of the two methods.

If a nucleus with spin I and magnetic moment $\underline{\mu}$ is placed in a magnetic field $\underline{H}_0$ it can easily be shown that the magnetic moment vector (or angular momentum vector) will precess with angular frequency

$$\underline{\omega}_0 = -g\left(\frac{e}{2Mc}\right)\underline{H}_0 \qquad (2.1)$$

where g is the so-called 'g-factor' or 'splitting-factor' of the nucleus in question and M is the mass of the proton, e and c having their usual significance. The value of $\underline{\omega}_0$ is independent of the angle between $\underline{\mu}$ and $\underline{H}_0$ and is called the Larmor precession frequency.

The potential energy associated with a magnetic moment

$\underline{\mu}$ in a magnetic field $\underline{H}_0$ is given by (apart from an additive constant)

$$E = -\underline{\mu} \cdot \underline{H}_0 = -\mu_{\parallel} H_0 \qquad (2.2)$$

where $\mu_{\parallel}$ is the component of $\mu$ along the direction of the magnetic field $\underline{H}_0$ and is given by

$$\mu_{\parallel} = g \left( \frac{e \hbar}{2Mc} \right) m \qquad (2.3)$$

where m is the magnetic quantum number m=I, I-1, .... - I. Therefore the energy associated with the state characterised by m is

$$E(m) = - g \left( \frac{e \hbar}{2Mc} \right) m H_0 \qquad (2.4)$$

Since the nucleus with spin I is subjected to a magnetic field the 'spin' vector has 2I + 1 allowed orientations and so the nucleus must have 2I + 1 energy levels accessible to it each fixed by a value of m. These levels are called Zeeman levels since they are similar to the Zeeman levels found in atomic physics.

By further analogy with atomic physics we can introduce the Bohr frequency condition

$$h \nu = \Delta E \qquad (2.5)$$

and postulate transitions between these Zeeman levels subject to the selection rule $\Delta m = \pm 1$ . Therefore combining eq. (2.4) and (2.5) and writing

$$\frac{e\hbar}{2mc} = \mu_n \quad \text{(definition of nuclear magneton)} \qquad (2.6)$$

the frequency emitted or absorbed by a nuclear dipole is given by

$$\hbar \nu_0 = g \mu_n H_0 \qquad (2.7)$$

and $\nu_0$ = Larmor frequency$/2\pi$. For magnetic fields obtainable in laboratories $\nu_0$ falls in the region 1 Mc/s to 40 Mc/s. Thus if a sample containing magnetic nuclei is subjected to both a steady magnetic field and radiation at the Larmor frequency transitions between the energy levels can occur with the absorption of energy from the applied radiation. This briefly is the process of nuclear magnetic resonance.

Since the transition probabilities for emission and absorption are equal a net absorption of energy will occur only if there is a majority of nuclei in the lower energy levels. In this thesis the magnetic nucleus of interest is the proton with $I = \frac{1}{2}$. Hence there are $2I + 1 = 2$ energy levels corresponding to $\mu$ parallel or antiparallel to the magnetic field $H_0$ , the parallel position

corresponding to the state of lower energy. The population of the two energy levels follows a Boltzmann distribution so that there is a surplus of nuclei in the lower energy state. This surplus can only be maintained if there is some mechanism whereby nuclei which have been pushed up into the higher energy state can 'relax' into the lower energy state. This mechanism is called 'Spin-lattice Relaxation' and is a process whereby energy is exchanged between the nuclear spins and the lattice. This process is characterised by a 'spin-lattice relaxation time' $T_1$ which can be regarded as a measure of the efficiency of the interaction between the spins and the lattice.

As long as the spin system does not saturate i.e. when the spin-lattice relaxation cannot maintain the population difference of the energy levels against the applied radiation, then a net absorption of energy by the spin system will occur. It is from a study of the absorption line shape and the relaxation time that information concerning molecular and crystal structure and molecular motion is obtained.

In order to understand fully the work reported here, it is now necessary to examine the absorption spectrum and the spin-lattice relaxation process in greater detail.

2.2. Spin - Spin Interaction.

As discussed in the previous section, a substance containing magnetic nuclei which is subjected to a strong magnetic field displays a resonance absorption at some radio frequency. As illustrated by Eq. 2.7 the frequency at which this absorption takes place depends only on the strength of the magnetic field and the so-called g-factor of the nuclei in question. Therefore in the ideal case of a system of isolated spins the magnetic absorption spectrum would consist of an infinitely narrow single line. However, ideal cases, as in most branches of physics, are strangers to the field of nuclear magnetic resonance and this simple picture is modified greatly by various mechanisms.

For any one type of magnetic nucleus from Eq. 2.7 the frequency at which absorption takes place depends entirely on the magnetic environment of the nuclei. Therefore, if, in the system of nuclei, the 'effective' magnetic field

varies from point to point, different nuclei will find themselves in different magnetic fields and resonance will occur over a band of frequencies. In practice it is found that all resonance lines are broadened out over a certain band-width due, in the main, to an inhomogeneous magnetic field in the sample. The cause, however, of this inhomogeneity may vary for different samples.

In crystalline solids the breadth of the resonance line is almost entirely due to interactions among neighbouring spins. If a crystalline sample is placed in a magnetic field then the total field experienced by any one nucleus consists of the constant applied field $H_o$ plus local magnetic fields produced at the nucleus by the magnetic moments of neighbouring nuclei. This can be expressed by the equation

$$\underline{H}_{effective} = \underline{H}_o + \underline{H}_{local} \qquad (2.8)$$

These neighbouring nuclei can be considered as small magnetic dipoles (in this thesis we are only concerned with protons, $I = \frac{1}{2}$) of magnetic moment $\mu$ and thus will depend on the relative dispositions of these dipoles. $|\underline{H}_{local}|$ depends on $\mu/r^3$, where r is the inter-nuclear distance, and is generally of the order of a few gauss .

Since the interaction between neighbouring magnetic nuclei falls off as the inverse cube of the distance separating them, any one nucleus is only affected by its nearest neighbours.

Considering now the simplest case possible, that of two interacting nuclei occuring asiisolated pairs it can be shown that $H_{local}$ varies as $(3\cos^2\theta - 1)$ where $\theta$ is the angle between $H_0$ and the line joining the two nuclei. Therefore, in the case of a system of isolated pairs of protons, the field at one proton can be written as

$$H_{effective} = H_0 \pm \alpha(3\cos^2\theta - 1) \qquad (2.9)$$

where the $\pm$ sign accounts for the two possible values of the component of the partner's magnetic moment in the direction $\underline{H}_0$ and $\alpha$ is a parameter which depends on r, the separation of the protons. This picture gives a pair of resonance lines symmetrically disposed about the frequency at which a simple resonance would occur. By measuring the line separation for such a system of proton pairs the distance between the protons could be measured and therefore some idea of the positions of the protons in the crystal lattice could be obtained. Excellent agreement between the above theory and experiment was found by Pake (1) in a single crystal of gypsum, $CaSO_4 \cdot 2H_2O$, when allowance was made

for the small broadening effects of magnetic neighbours outside each proton pair. Similar methods have been used by Itoh et alia on several other single crystal hydrates e.g. reference (2). It will be seen later that in the case of Urea the protons approximate to a two-spin system and that a useful check on the proton configuration can be obtained by measuring the splitting of the observed resonance line.

It is important to note that the nuclear configuration considered so far has been regarded as rigid in so far as the positions of the nuclei are effectively stationary for times of the order of $10^{-4}$ seconds. It is well known that if the lattice is rigid by this criterion, then the shape and width of the absorption line hardly differs from that which would arise from a completely stationary arrangement.

2.3. Second Moment and Molecular Structure.

The addition of even one more nucleus to the interacting pair considered in the last section increases the complexity greatly and the general spectrum of N(N>4) interacting spins more or less defies solution. For simple cases containing not more than three nuclei per unit interaction cell detailed perturbation calculations can be made and

examples of this type of work are given in references 3,4, and 5. An elegant analysis of the experimental data from the line structure is possible, however, due to a theory developed by Van Vleck (6). This theory relates nuclear orientation and the mean square width of the absorption lines. For any postulated spin configuration the so-called 'second moment' of the line shape can be calculated. The second moment is defined as the mean value of the square of the frequency deviation from the centre of resonance, the average being taken over the shape function.

The line shape is taken to be a function $g(\nu)$ so normalised that

$$\int_{-\infty}^{\infty} g(\nu)\, d\nu = 1 \qquad (2.10)$$

Then if $\nu_0$ is the resonance frequency, the second moment is

$$\langle (\Delta\nu)^2 \rangle_{av.} = \int_{-\infty}^{\infty} (\nu - \nu_0)^2 g(\nu)\, d\nu \qquad (2.11)$$

Technically the magnetic field $H_0$ is varied in magnetic resonance as opposed to varying the frequency of the applied radiation and so it is convenient to express the

second moment in terms of gauss$^2$.

$$\text{Second moment} = \langle (\Delta H)^2 \rangle_{av} = \tfrac{3}{2} I(I+1) N_R^{-1} g^2 \mu_n^2 \sum_{j>k} (3\cos^2\theta_{jk} - 1)^2 r_{jk}^{-6}$$

$$+ \tfrac{1}{3} N_R^{-1} \mu_n^2 \sum_j \sum_f I_f (I_f+1) g_f^2 (3\cos^2\theta_{jf} - 1)^2 r_{jf}^{-6} \quad (2.12)$$

where $\langle (\Delta \nu)^2 \rangle_{av.} = g^2 \mu_n^2 \hbar^{-2} \langle (\Delta H)^2 \rangle_{av}$

The symbols in Eq. (2.12) are defined below :

- $g, I$ Nuclear g-factor and spin of the nucleus at resonance
- $g_f, I_f$ Nuclear g-factors and spins of the other nuclear species in the sample
- $r_{jk}$ Length of the vector joining nuclei j and k
- $N_R$ Number of nuclei at resonance which are present in the group to which broadening interactions are considered to be confined in evaluating $\langle (\Delta H)^2 \rangle_{av.}$

For a polycrystalline sample where the constituent microcrystals are randomly distributed the factor $(3\cos^2\theta_{jk} - 1)$ is averaged over a sphere and the expression for the second moment reduces to

$$\langle (\Delta H)^2 \rangle_{av} = \tfrac{6}{5} I(I+1) N_R^{-1} g^2 \mu_n^2 \sum_{j>k} r_{jk}^{-6}$$

$$+ \tfrac{4}{15} \mu_n^2 N_R^{-1} \sum_j \sum_f I_f (I_f+1) g_f^2 r_{jf}^{-6} \quad (2.13)$$

Both formulae have been used successfully (see references 3, 4, 7 ) before and both have been used in obtaining the results reported here.

In the case of the proton, where the spin and g-value are known, computation of the theoretical second moments merely involves a knowledge of the lengths and orientations of the inter-nuclear vectors. Experimental second moments can be found from the experimental line shapes, as shown by Pake and Purcell (8) and comparison with theoretical values can confirm or deny any assumed structure.

In general, the most information is obtained by a study of line shape combined with the angular dependence of the second moment in single crystals and is illustrated in the sections dealing with Urea.

2.4. Spin-lattice Relaxation.

Before a sample is placed in the magnetic field $H_o$ the magnetic nuclei are randomly orientated and the Boltzmann factors for the various energy levels are almost unity (not quite due to the presence of the earth's magnetic field). Thus when the sample is thrust suddenly into the field some of the nuclei in the higher energy states must get rid of some energy to restore equilibrium. They do so by giving up energy to other degrees of freedom in the system i.e. to the 'lattice'. The actual mechanism of this 'relaxation process' is relatively unimportant in the

problems to be discussed. It is, perhaps, sufficient to state that this process is not due to normal thermal vibrations of the lattice and that Bloembergen et alia (9) showed that more general types of lattice motion, when excited, are effective in bringing about spin-lattice relaxation.

The establishment of equilibrium follows an equation of the form

$$n = n_0 \left(1 - e^{-\frac{t}{T_1}}\right) \qquad (2.14)$$

for nuclei of spin $\frac{1}{2}$ where n is the existing difference in population between the two levels and $n_0$ is the equilibrium value of this difference. $T_1$ is defined as the 'spin-lattice relaxation time' and is the time required for all but $1/e$ of the equilibrium excess number to reach the lower energy state. Thus $T_1$ can be regarded as a measure of the interaction between the nuclear spins and the lattice. The value of $T_1$ is characteristic of the sample and ranges from $10^{-4}$ to $10^{4}$ sec. for different materials and conditions. Since the relaxation process arises from lattice motion it is not surprising that a study of $T_1$ should provide information about such motion.

Taking the process one step further a study of $T_1$ yields

information about group reorientations in solids which displace the nuclei much more than thermal vibrations and so lead to short values of $T_1$. Examples of this type of work are given in references (10,11.)

Eq. (2.14) can be written in the form

$$\frac{dn}{dt} = \frac{n_0 - n}{T_1} \qquad (2.15)$$

where $\frac{dn}{dt}$ is the rate of approach to equilibrium. Taking into account the effect of the applied radiation which induces transitions to the higher energy state, this leads to

$$\frac{dn}{dt} = \frac{n_0 - n}{T_1} - 2n W_{\frac{1}{2} \to -\frac{1}{2}} \qquad (2.16)$$

where $W_{\frac{1}{2} \to -\frac{1}{2}} = \frac{1}{4} \gamma^2 H_1^2 g(\nu)_{max.}$

and represents the probability of a single transition (the factor 2 arises since the excess number n changes by 2 for each transition). In the above expression $\gamma$ is the nuclear gyromagnetic ratio, $2H_1$ is the amplitude of the applied radiation and $g(\nu)_{max.}$, the maximum value of $g(\nu)$, is expressed in terms of a quantity $T_2$

$$T_2 = \frac{1}{2} g(\nu)_{max.} \qquad (2.17)$$

$T_2$ is the so-called 'spin-spin relaxation time' and, as defined by Eq. (2.17), is a measure of the inverse line width of the absorption line.

In the steady state i.e. $\frac{dn}{dt} = 0$ a combination of the above equations yields

$$\frac{n}{n_0} = \frac{1}{1 + \gamma^2 H_1^2 T_1 T_2} \qquad (2.18)$$

which shows that the absorption intensity is reduced by a factor $[1 + \gamma^2 H_1^2 T_1 T_2]^{-1}$ in presence of the applied radiation, assuming that the intensity is proportional to the excess number n. Eq. (2.18) leads to a method of measuring $T_1$ as will be seen in the section dealing with Rochelle Salt. The above theory is developed fully in reference (9).

A combination of line-width study with that of spin-lattice relaxation time variation can give valuable information about molecular or atomic reorientations in solids (see references 12, 13) and an approach of this type was made on Rochelle Salt (see later) in studying the ferroelectric properties of this crystalline solid.

2.5. Summary.

In this section the general theory of nuclear magnetic

resonance has been reviewed and some indication given as to the method of application to the problems discussed in later sections. Any further theory required will be given in the appropriate section.

## SECTION 3.

# 3. APPARATUS.

## 3.1. Introduction.

From the general resonance equation developed in Section 2.1. viz

$$h\nu_0 = g\beta_N H_0$$

it can be seen that, for resonance absorption to occur, the sample must be placed in a magnetic field $H_0$ and subjected to electromagnetic radiation at the resonant frequency $\nu_0$. Hence the main requirements for work in this field appear to be a magnet, a source of electromagnetic energy and some means of detecting the absorption of this energy.

However, due to the Boltzmann distribution, the excess number of nuclei in the lower energy state, which cause the absorption, is very small. In fact, in the case of protons at room temperature in a field of 20,000 gauss for every million protons in the upper energy state there are one million and fourteen in the lower energy state. This means that nuclear magnetic resonance will produce relatively weak effects and sensitive equipment will be required for their detection.

Several methods have been developed and they are described fully elsewhere (see, for example, references 9, 14,15,16). Each method has its advantages and its limitations and tends to have been developed according to the needs of the problem on hand. As the work of this laboratory had, in the main, been concerned with fields

where relatively broad absorption lines were obtained, a radio-frequency bridge system had been built. This apparatus was constructed by Dr. R.G.Eades (17). Some alterations were made to the equipment and these will be described in detail later on. In the following section a brief description is given of the nuclear magnetic resonance apparatus as a whole.

3.2. General Set-up for detecting Nuclear Magnetic Resonance

The actual detection of nuclear magnetic resonance can, in certain cases, be realised by quite simple apparatus. One such set-up (18) required that the sample be placed in a coil which formed part of a tuned circuit. The coil, situated in the magnetic field $H_o$ was connected, through a high impedance, to a signal generator so that the circuit was supplied by a constant current. If the signal generator frequency is fixed and the field $H_o$ adjusted to its resonant value then the nuclear absorption causes a change in the parallel impedance of the circuit which is detected by the change in voltage caused across the circuit. This process is the basis of most experimental methods developed so far.

The radio-frequency bridge system used for the work reported here is similar to the arrangement used by Bloembergen et alia (9). A schematic diagram of the

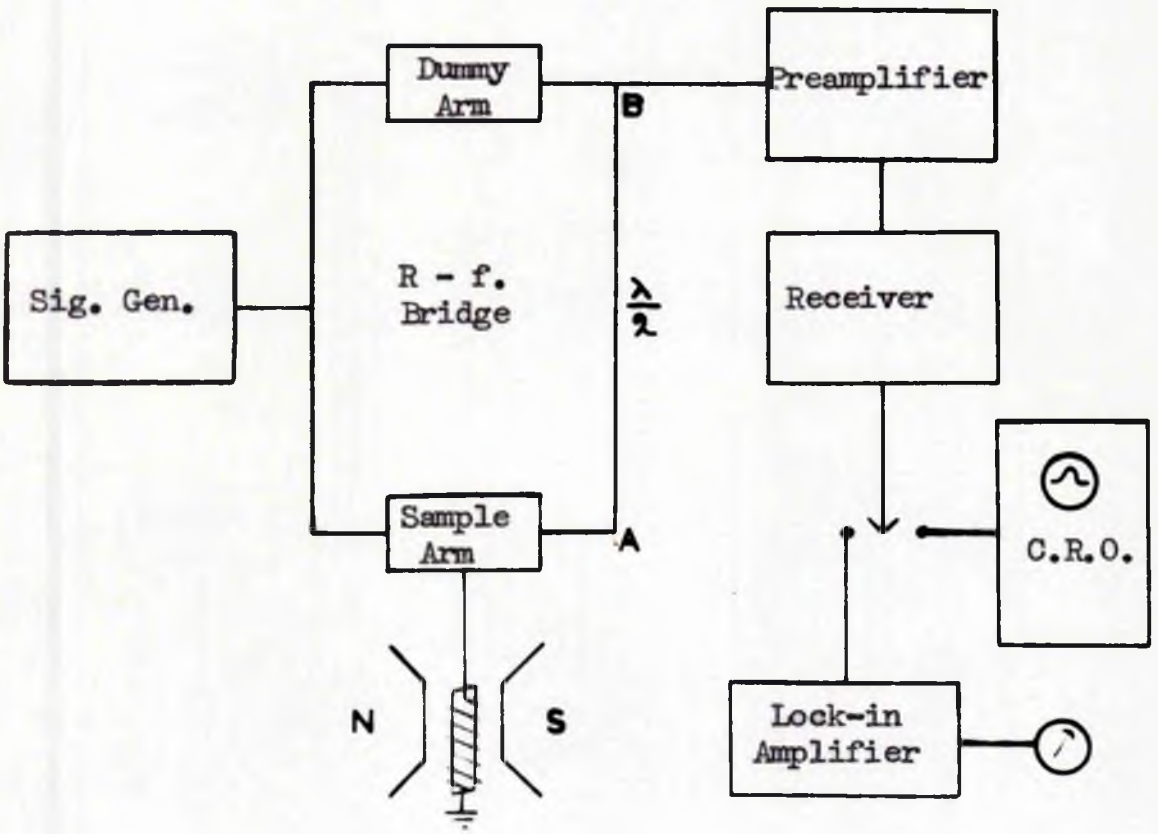
Dummy Arm
Preamplifier
B
Sig. Gen.
R - f. Bridge
λ/2
Receiver
Sample Arm
A
C.R.O.
N
S
Lock-in Amplifier

FIGURE 1.

apparatus is shown in Figure 1. The sample is placed in the radio-frequency coil of the tuned circuit in one arm of the bridge, the coil being so arranged that its axis is perpendicular to the magnetic field $H_o$. The main field $H_o$ can be varied in two ways. By means of field bias coils it is possible to alter tha value of $H_o$ so that the effective range of the magnet approximately is $H_o \pm 30$ gauss. Thus by choosing the appropriate frequency the magnetic field can be varied over this range until the resonant condition is fulfilled. $H_o$ is also modulated with a small amplitude by means of a pair of Helmholtz coils so that when $H_o$ is properly adjusted, resonance is swept through at the frequency of the modulation which is in the low audio-frequency range. This results in an a.f. modulation of the radio-frequency signal supplied by the oscillator. After rectification, the resulting audio signal is either displayed on the C.R.O. screen or passed on to a narrow-band amplifier depending on the type of resonance line being studied. In the case of a resonance line obtained from a liquid i.e. a narrow line, the output from the receiver is applied to the Y-plates of the C.R.O., the X-plates being fed with a sinusoidal voltage at the modulation frequency properly

phased relative to the modulation voltage. In this way the resonance line is traced out on the screen as a function of the magnetic field $H_o$. For the observation of broad-lines - in general lines obtained from solid samples are broad - the field $H_o$ is modulated at an amplitude which is a small fraction of the line-width and the resulting signal is passed on to a narrow-band phase sensitive detector, or 'lock-in' amplifier, where it is mixed with a sinusoidal voltage at the modulation frequency. By shifting the main field $H_o$ by known amounts it is then possible to plot the output of the lock-in amplifier against the applied field. Using this technique the first derivative of the absorption line is obtained but, as will be seen, this is no drawback to the interpretation of the experimental results. With the apparatus described here the plotting of the derivative is performed automatically since $H_o$ is varied continuously by means of a motor-driven potentiometer system and the output from the lock-in amplifier is fed into a recording microammeter. The main features of the radio-frequency bridge are that it balances out the signal generator fluctuations and effectively increases the depth of modulation. In Figure 1, AB

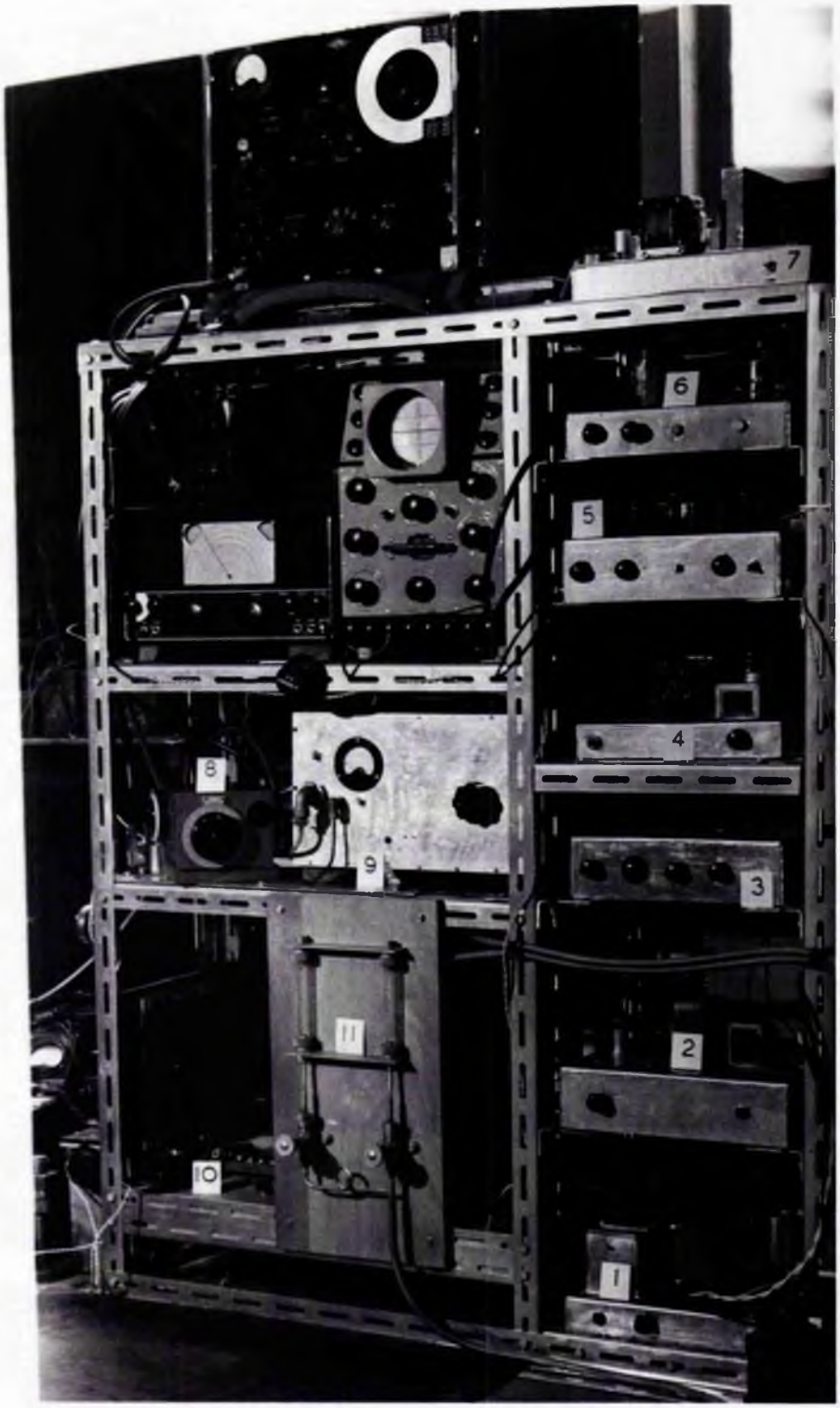


FIGURE 2.

represents an extra half wavelength of cable which is included to give a voltage node at point B when the bridge is balanced. This half wavelength of cable, which is several metres long at the frequency used, is rather inconvenient and was eliminated during the work on Rochelle Salt when a different type of bridge was used.

In order to clarify certain aspects of the equipment more detailed information about specific parts is given below.

3.3. Details of Apparatus.

3.3.1. General.

Figure 2 is a photograph of all the electronic stages of the apparatus. The various parts are numbered as follows:

(1) Power supply for the 25 c/s generator and the Power Amplifier.

(2) The Power Amplifier delivering power to the modulation coils.

(3) 25 c/s generator.

(4) Power supply for the Lock-in Amplifier.

(5) The Lock-in Amplifier.

(6) Phasing and transforming unit supplying the X-sweep for the C.R.O.

(7) Power supply for the receiver and the preamplifier.

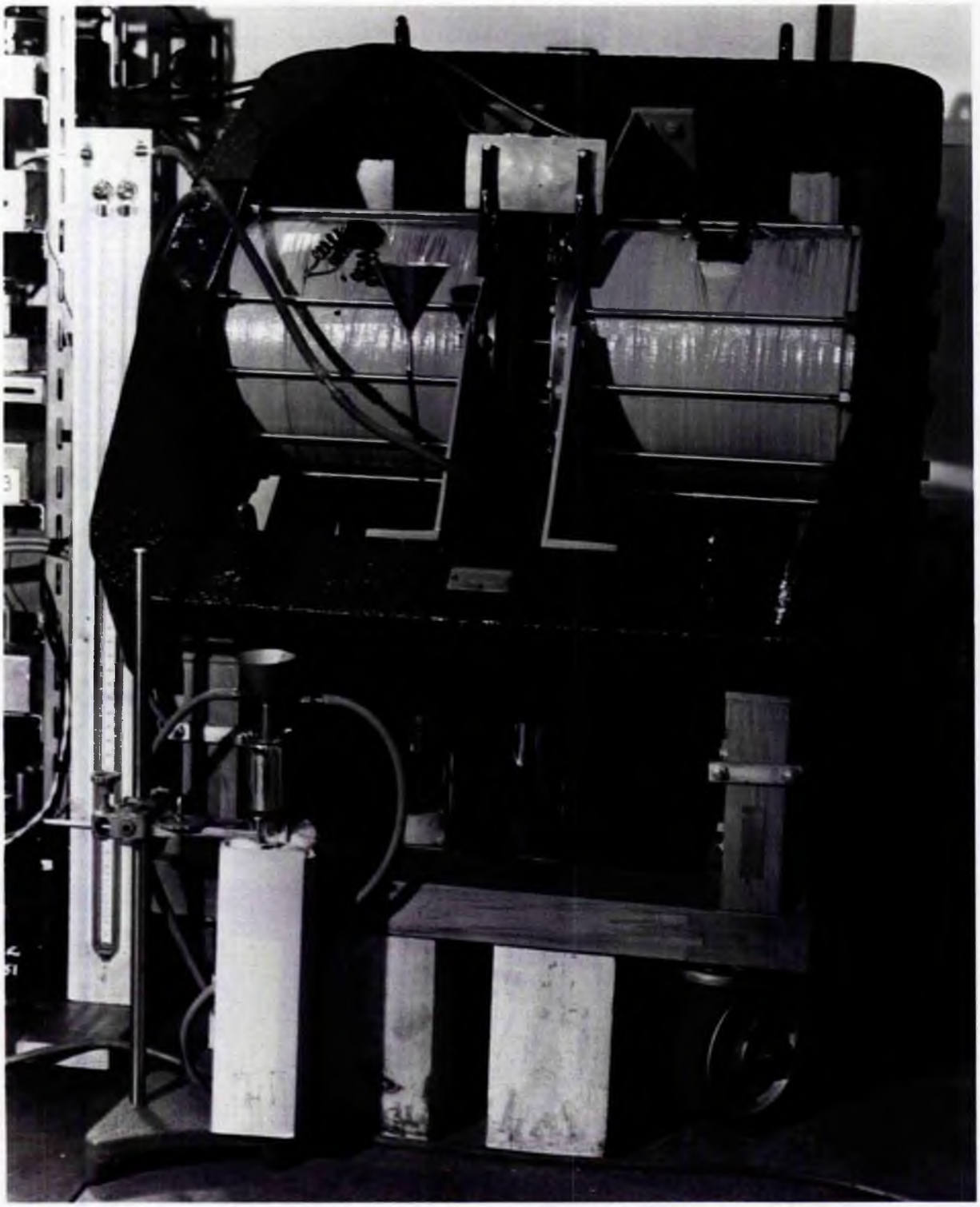

FIGURE 3.

(8) The 'dummy' unit of the r.f. bridge.

(9) R.f. preamplifier feeding the receiver in order to improve the noise figure.

(10) Power supply for the Signal Generator.

(11) Control valves for the flow gas used in varying temperature of the sample.

Also shown on the photograph are the Signal Generator (top left), the receiver and the C.R.O.(below the Signal Generator).

Figure 3 shows the large permanent magnet used in all the experiments. The gas cryostat system can just be discerned beneath the magnet.

3.3.2. The Magnet.

The specifications of the magnet are :

Pole face diameter : 8 ins. Gap width : 2 ins.

Field : 5500 gauss Field homogeneity in best region : 0.25 gauss/cc.

The magnet was designed by Drs. Andrew and Rushworth and the pole caps were fitted with special ring shims (19) to obtain a highly uniform field. The original magnetising coils are still in place and are used as the field bias coils.

3.3.3. The Radio-frequency Section

This part of the apparatus consists of a Signal

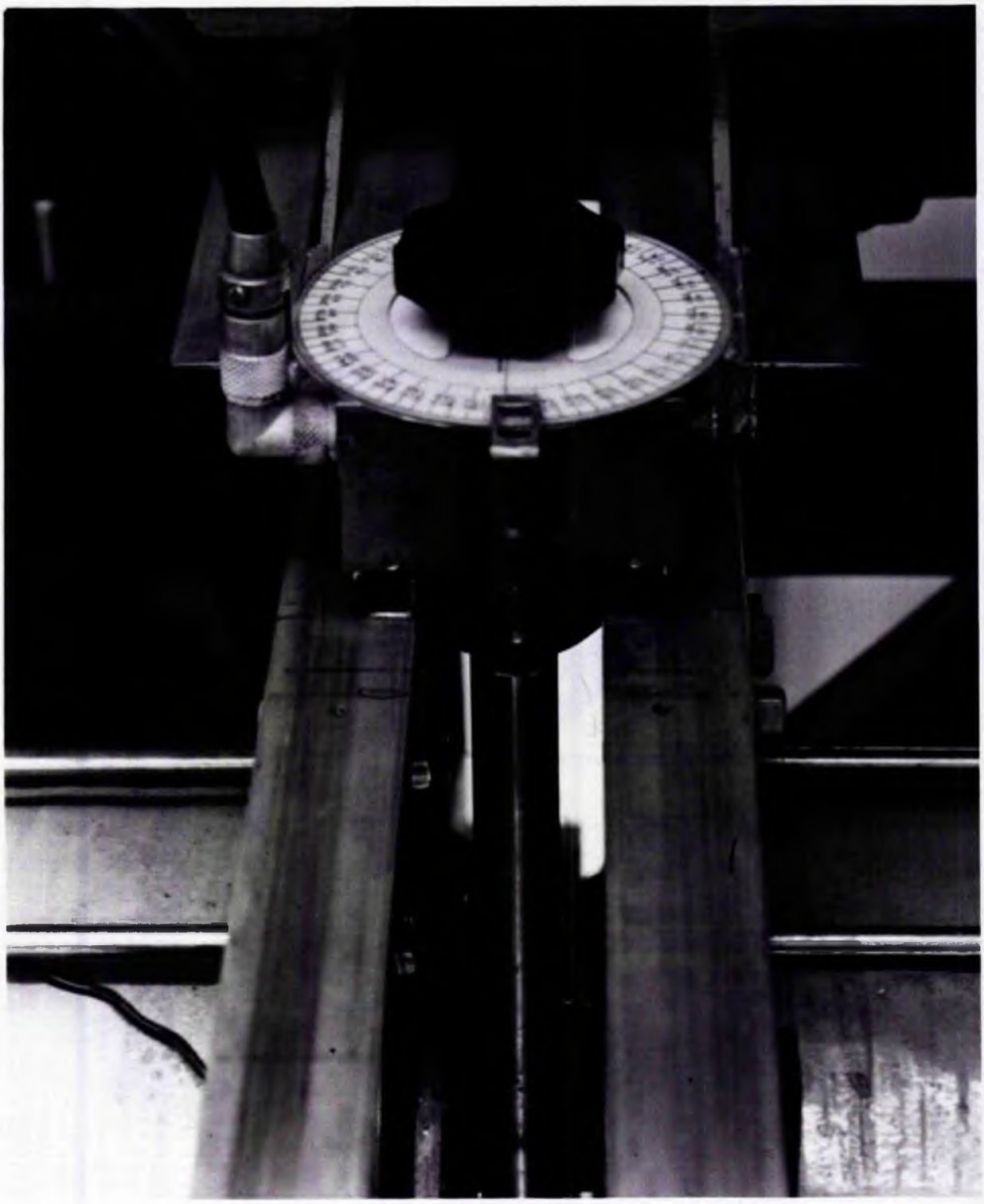

FIGURE 4.

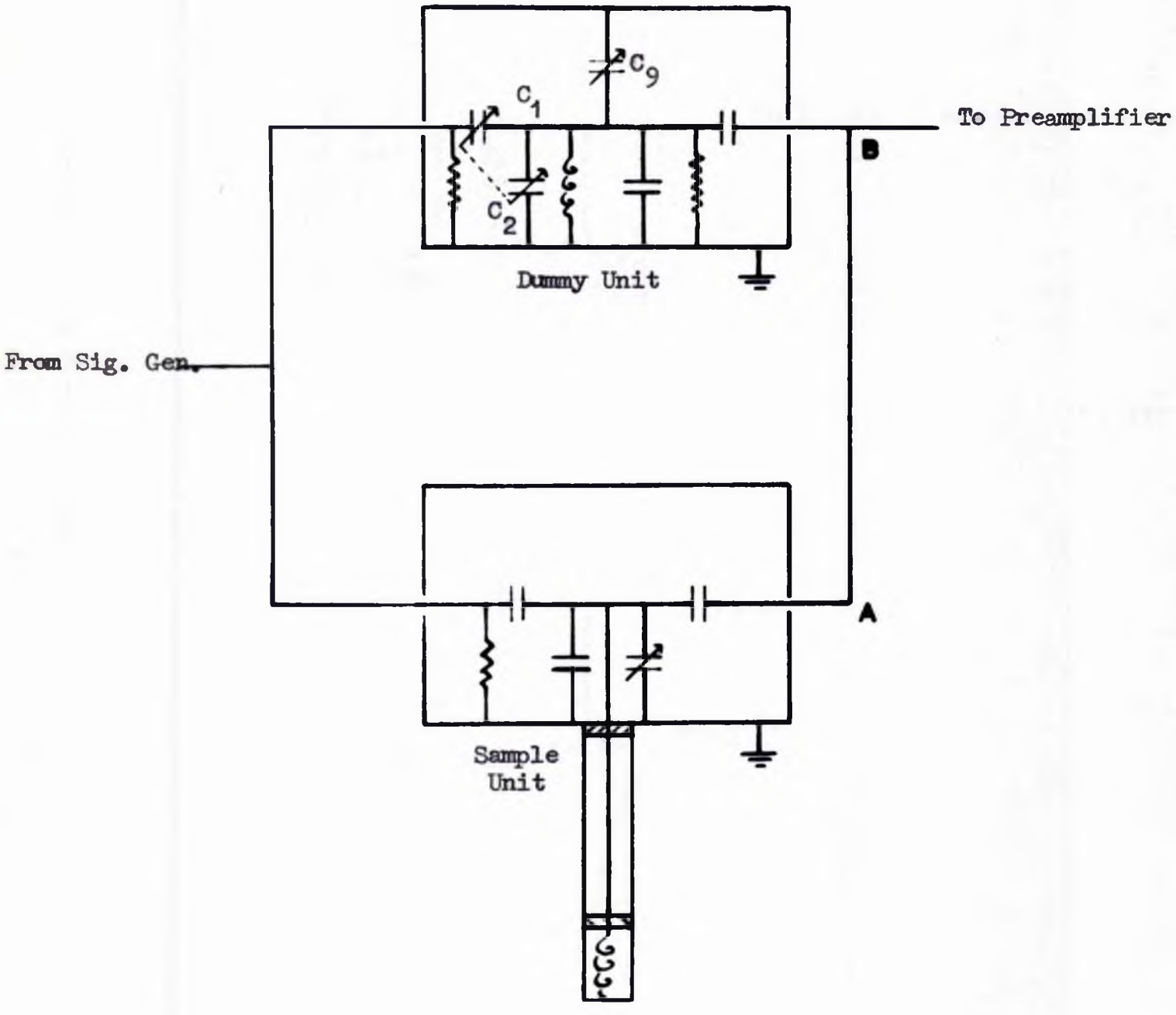
$C_9$
$C_1$
To Preamplifier
B
$C_2$
Dummy Unit
From Sig. Gen.
A
Sample
Unit

FIGURE 5.

Generator, a r.f. bridge, a preamplifier and a receiver. The Signal Generator and the receiver are both commercial instruments, the only modifications being the use of a D.C. supply for the valve heaters and stabilised H.T. power supplies. The power supplied to the preamplifier is also stabilised. This unit, employing an aligned grid pentode, gives a useful gain with a large improvement in signal to noise ratio.

The r.f. bridge used during the work on Urea was of the type described in reference 9. It consisted of two units connected together by low impedance cable. The dummy unit can be seen in Figure 2 while the unit containing the sample is seen in Figure 4. The circuit of the bridge is shown in Figure 5.

The mechanical stability of this bridge was very good and the bridge balance was stable up to 40db. This was ensured by using heavy gauge copper wire for connecting components and making certain of good bonding between units. Pake (20) has shown that if the signals arising from the two arms of the bridge are balanced in phase and unbalanced in amplitude then a nuclear magnetic resonance absorption line is obtained (if the balance conditions are reversed a dispersion curve arises). As all

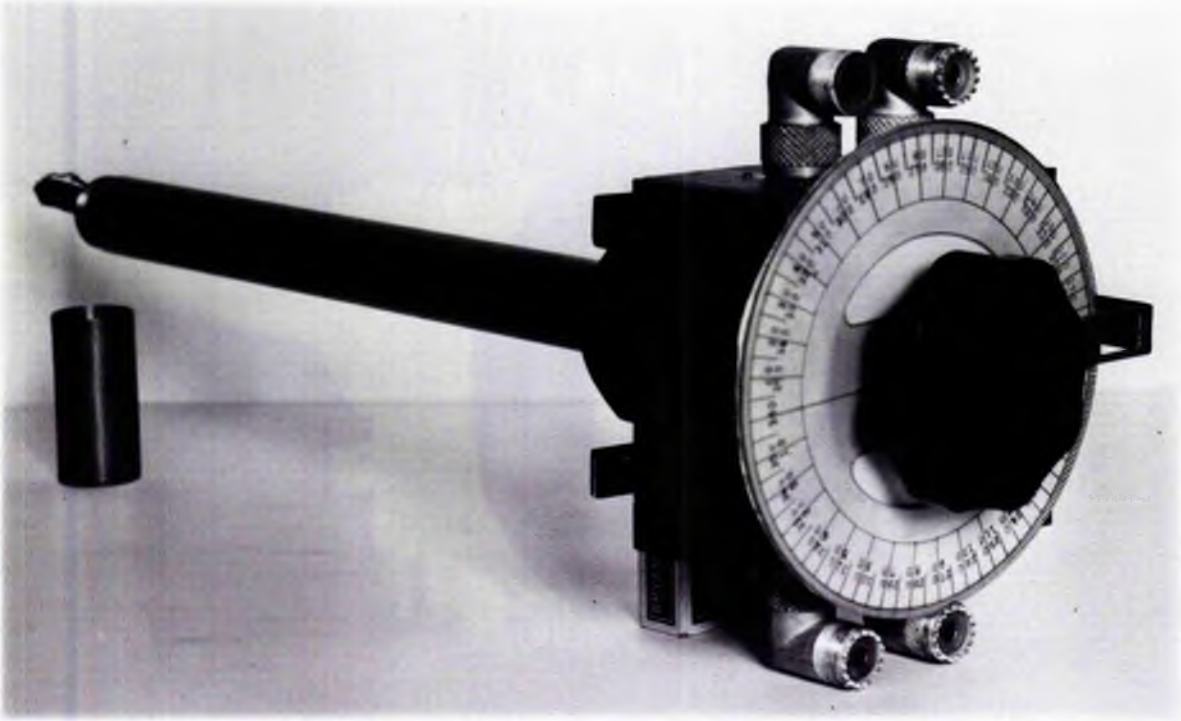

FIGURE 6.

measurements are made from absorption curves the half wavelength of cable AB is included in one arm of the bridge to give approximate phase balance, the final adjustment being made with the small trimming condenser $C_9$. The ganged pair $C_1$ and $C_2$ are arranged 180° out of phase to give an approximately phase independent amplitude control.

All the measurements on Urea were made with a single crystal whose orientation with respect to the applied field was varied. Since the crystal was situated in a close-fitting r.f. coil, any rotation of the crystal was accompanied by a rotation of the coil and therefore, to eliminate any sliding contacts in the bridge, a unit was built so that the entire sample arm of the bridge could be rotated. This unit is shown in situ in Figure 4 and in more detail in Figure 6. The r.f. coil, containing the crystal, is situated at the end of a brass tube 30 cms. long and 2.5 cms outside diameter. A screw-cap is placed over the coil so that it is completely screened.

This is very important as it was found that any unscreened part of this bridge arm tended to pick up spurious 25 c/s signals from the modulation coils resulting in prohibitive distortion of the desired signal.

The cap, coil and tube are clearly seen in Figure 6. The tube was mounted at right angles to a brass box which contained the circuit parameters which, together with the coil, comprised the sample arm of the bridge. Connection was made to the coil by means of a thick copper wire which ran the length of the tube, insulating spacers being used to prevent shorting. The spacer nearest the coil was made of Teflon which does not contain hydrogen and thus does not give rise to any unwanted signal. The tube fitted closely into a brass collar attached to which were two small brass rails (see Figure 6). It was possible to rotate the tube with respect to the collar and any desired position could be obtained by clamping the tube by means of a screw fitted in the collar. The angle turned through could be read off a scale fitted to the box - a pointer having been attached to the collar (see Figure 4). When the tube was placed in the magnet gap the two small rails on the collar sat on larger rails fixed to the magnet (see Figure 4) and the construction was such that the tube was perpendicular to the magnetic field and that the position of the collar was fixed relative to the field. Summing up it will be seen that with this arrangement, it was possible to rotate the

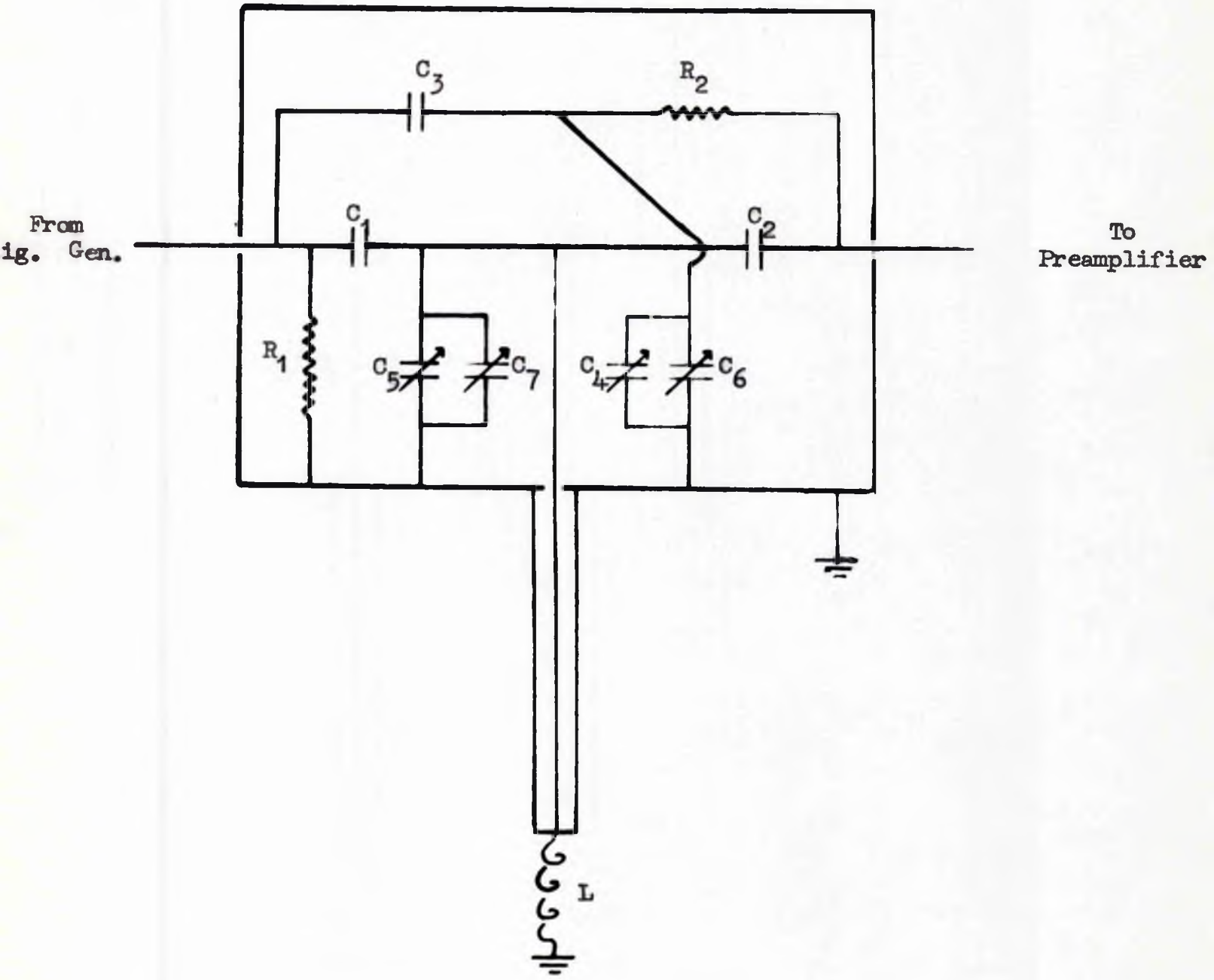


FIGURE 7.

crystal through a definite angle with respect to the field.

3.3.4. The Twin 'T' Bridge.

The bridge system described in the previous section has one or two disadvantages which are of importance when dealing with weak signals. The two arms of the bridge must be matched which entails great care in the selection of components. The number of components plus the fact that long lengths of co-axial cable are used (e.g. the extra half wavelength) make it well nigh impossible to realise a high Q-factor. In order to improve the Q of the bridge a twin 'T' bridge (21) was constructed. This has the advantages that it is a single unit, it eliminates the half wavelength of cable and it is much simpler to build.

The circuit for the bridge is shown in Figure 7. The bridge components were contained in a box made of $\frac{1}{8}$th inch brass sheet - heavy gauge copper wire being used for all internal connections to ensure mechanical rigidity. The tube leading down to the r.f. coil was made of german-silver since a metal of low thermal conductivity was deemed necessary as the sample (this

bridge was used during work on Rochelle Salt) had to be taken through a specific temperature range. A glass capillary rod was cemented inside the metal tube to enable a wire to be led down to the r.f. coil. The tube plus coil fitted into a long Dewar tube situated between the poles of the magnet so that experiments with varying temperature could be carried out.

This type of bridge has the added advantage that the phase and the amplitude balance are controlled independently by the condensers $C_5$ and $C_4$, respectively.
The balance conditions are (22)

Phase balance : $$\frac{1}{\omega^2 L} = C_5 + C_1 + C_2\left(1 + \frac{C_1}{C_3}\right)$$

Amplitude balance : $$\frac{1}{R} = \omega^2 C_1 C_2 \left(1 + \frac{C_4}{C_3}\right) R_2$$

where R is the equivalent shunt resistance of the coil and $\omega$ is the angular frequency of the electromagnetic radiation supplied to the bridge. The condensers used in this bridge were of the ordinary small variable air type, $C_6$ and $C_7$ being small trimmers consisting of one fixed vane and one movable vane. This bridge could be balanced satisfactorily to 1 part in $10^3$ but 1 part in $10^2$ was sufficient for the experiments performed.

The Q-factor of the circuit in situ was approximately 60.

3.3.5. The Low-frequency Section.

This part of the apparatus consists of the 25 c/s oscillator, the Lock-in amplifier, the Power amplifier and their associated power supplies.

The 25 c/s oscillator supplies the drive voltage for the field modulating equipment and the reference signal for the Lock-in amplifier. It consists of a multivibrator stage followed by two tuned amplifiers. The output consists of a good sinusoidal waveform which has approximately a 3% total harmonic content as checked on a Muirhead Frequency Analyser.

The Lock-in amplifier is of a convential type (23). The band-width of the amplifier is of the order of 0.25c/s centred about 25 c/s. As stated previously the Lock-in amplifier is used for tracing out the first derivatives of broad absorption lines. The first derivative can either be put on a visual meter or on a recording meter. In order to obtain the best results a large time constant was incorporated in the output stage of the amplifier. Since it is a D.C. voltage output which is obtained, random noise voltages are likely to affect the output in either direction and

a large time constant tends to make the resultant fluctuation zero. The ultimate value of the output time constant depends on the field scanning rate (see Section 3.2.) so that for broad lines it is advantageous to scan as slowly as possible in order to have as large a time constant as possible.

The Power amplifier is of the Williamson type (24) and is capable of delivering 15 watts at 25 c/s to the modulation coils. These coils, each consisting of 1000 turns of 22 s.w.g. wire, can be seen in position in Figure 8.

During the course of this work it was necessary to calibrate the field scanning system occasionally. This was done in the following manner :

A liquid sample was placed in the coil so that a narrow resonance line was displayed on the screen of the C.R.O. With no current flowing through the field coils the frequency of the signal generator was varied until the resonance line was accurately centred in the middle of the screen. The frequency of the signal generator was then determined using a heterodyne frequency meter (observed by beating the two signals on the C.R.O. screen).

Known values of current were then passed through the field coils and the process repeated. Since the current through the coils is registered as a voltage drop across a standard resistance, the above results gave a value of the frequency shift per unit voltage drop i.e. frequency shift per unit current through the field coils. The measurements were repeated several times and the Method of Least Squares used in determining the result. Using Bearden and Watt's values (25) for

Planck's constant, $h = 6.62363 \times 10^{-27}$ erg. sec.

Magnetic moment of proton, $\mu = 1.521026 \times 10^{-3} \mu_e$

1 Bohr Magneton $= 9.2710 \times 10^{-21}$ erg. gauss$^{-1} = \mu_e$

in the equation

$$h\nu = 2\mu H,$$

the frequency shift per millivolt was converted into field shift per millivolt measured in units of gauss/mV.

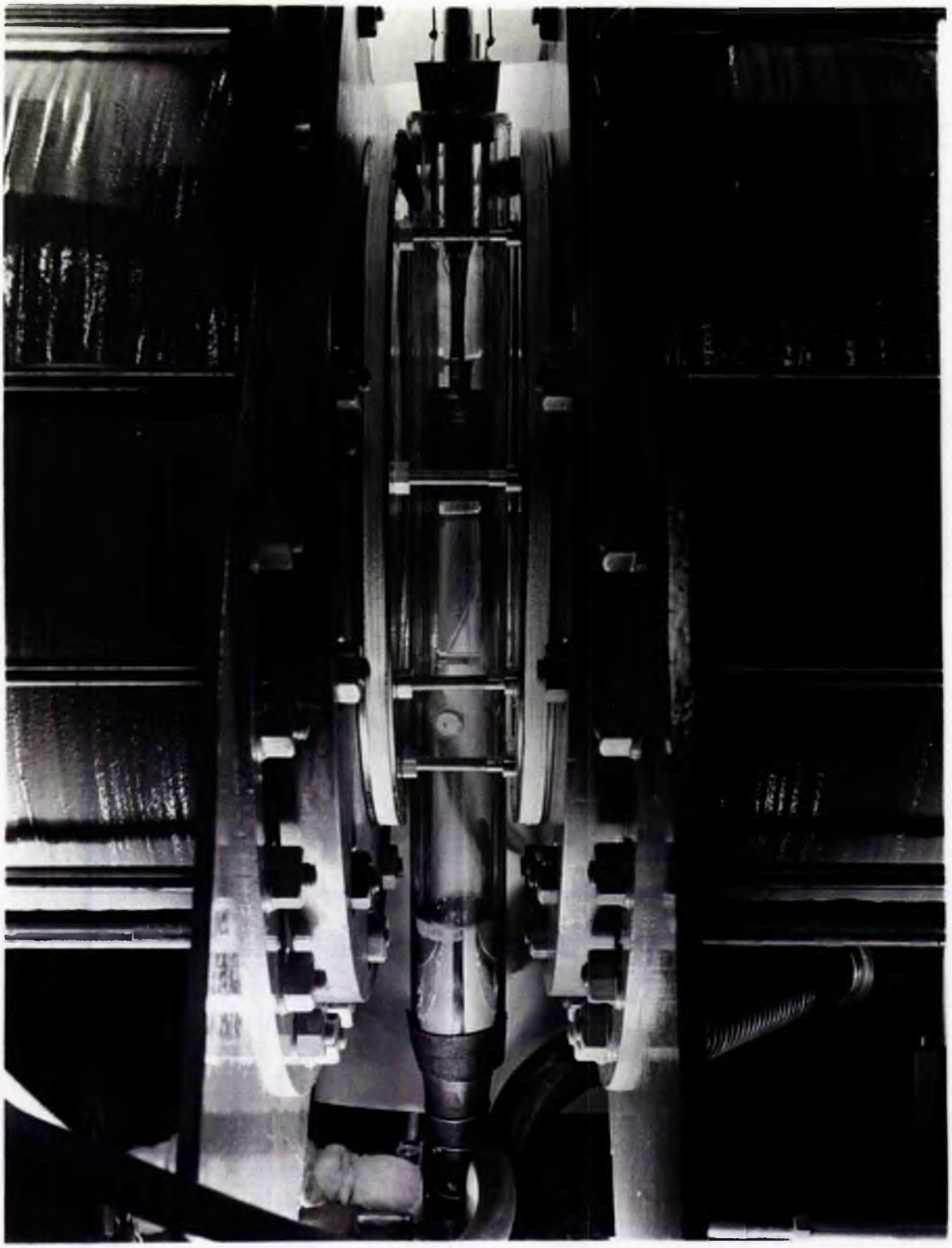

FIGURE 8.

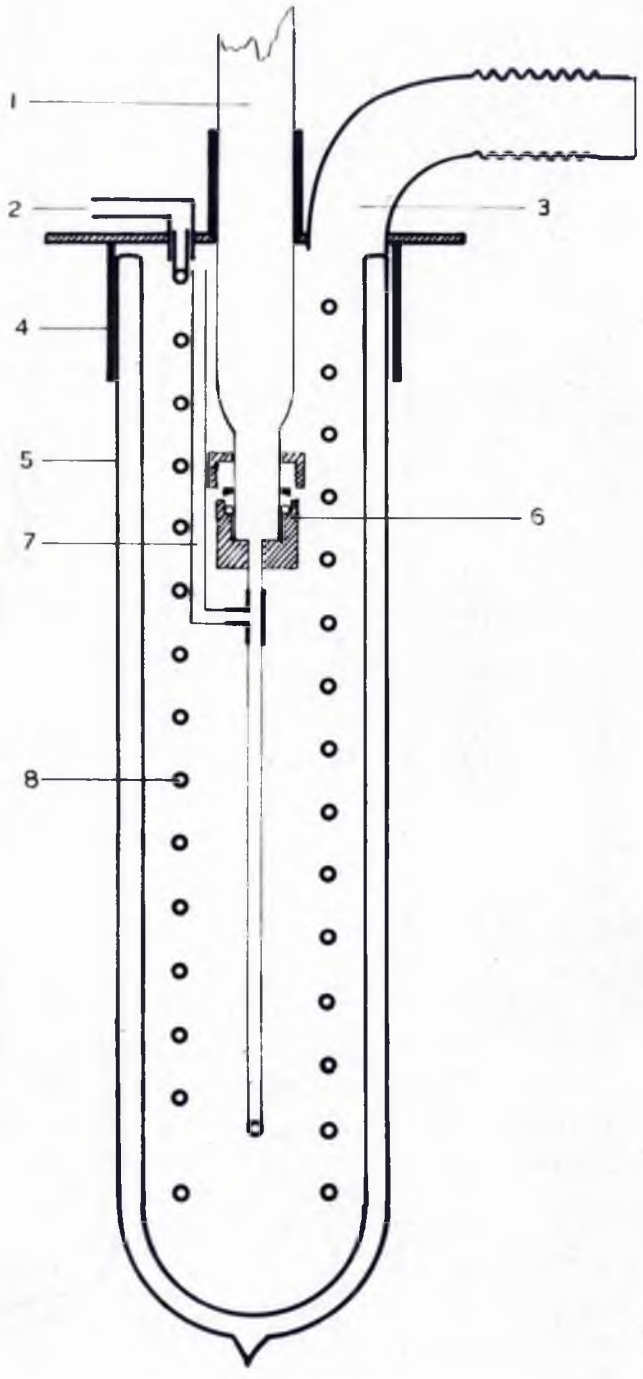


GAS CRYOSTAT.

FIGURE 9.

3.4. Temperature Regulation

In the course of the work on Rochelle Salt the temperature of the sample was varied over the range 200°K - 320°K. This was achieved by a gas-flow cryostat system. This method has the advantages that (a) the temperature can be held quite steady by the manipulation of a flow valve, and (b) a change from one temperature to another can be effected in 15 minutes.

Temperatures below 0°C were obtained in the following way:

Air was passed from a cylinder through a drying chamber to a flow gauge. Connection was made from the gauge so that the air could pass (1) through a cryostat (2) flow past the sample without being cooled (3) divide so that some air flowed through the cryostat and some did not. A cross-section of the cryostat is shown in Figure 9. The main Dewar (5) is filled with liquid air in which is immersed a german-silver tube spiral (8). The air from the flow gauge enters via (2) and is cooled in passing through the spiral. It then passes into the long Dewar tube (1) which is situated between the poles of the magnet and contains the r.f. coil with its

sample (see Figure 8). This Dewar is made tight with respect to the spiral by means of a Gaco ring seal (6). (4) is a rubber gasket which seals the main Dewar (5) to a brass top-plate and (7) is an inlet for air which is not required to be cooled. A pumping line (3) is included in the cryostat but this was never used as the temperature range available was quite sufficient for the work undertaken.

For work in the region 290°K - 320°K the flow gas was first heated before it entered the long Dewar tube by inlet (7). This was done by passing the gas through a length of glass tubing around which was wound a heater coil. The heater was supplied by a Variac transformer and, by a combination of heater voltage control and air flow regulation, temperatures up to 340°K could be obtained. Needless to say, in this temperature range no liquid air was put in the main Dewar (5).

Temperatures in the range 273°K - 290°K were best realised by a combination of cold and warm streams of air. As can be seen from Figure 9 the cold air (from (2)) and the warm air (from (7)) mix at the foot of the long

Dewar (1) and the mixture passes up the Dewar to cool the sample.

All temperature measurements were made with a copper-constantan thermocouple used with a Doran Thermocouple Potentiometer, the accuracy over the range used being about $\pm\frac{1}{2}C^{\circ}$.

Figure 8 shows the long Dewar tube in position between the pole faces and the brass top-plate of the cryostat assembly. Also visible are the modulation coils held apart by brass spacers - and the screening can of the r.f. coil.

One disadvantage of the above type of cooling (or heating) arrangement is that it is very wasteful in the sense that the flow gas is allowed to disperse into the atmosphere after use. This is not of great importance when air is used as the flow gas but if hydrogen or helium were used then it tends to become rather expensive. A more economical system is that with the variable heat leak and conduction cooling as used by Gutowsky(26).

## SECTION 4.

# 4. CRYSTAL GROWTH

## 4.1. Introduction.

In Section 2.3. the expression for the second moment of a microcrystalline powder is given (Eq. 2.13). Examination of the formula shows that only limited information concerning crystal structure is available. A combination of a given set of experimental results with theoretical results, calculated from Eq. 2.13 , yields only one structural parameter viz. r the inter-nuclear vector. Much more detail is obtainable from a study of single crystals as can be seen from Eq. 2.12 which, in addition to r, contains a factor $(3\cos^2\theta_{jk}-1)^2$ which depends on the orientation of the inter-nuclear vector $r_{jk}$ . Hence it should be possible to assign definite positions to the various nuclei in the crystal lattice. It is therefore obvious that single crystals are necessary if any detailed structure determination is to be attempted.

The initial problem in the work reported here was concerned with the crystal structure of Urea and therefore it was decided to develop some method of growing single crystals. Later on it became evident

that it would be advantageous to have single crystals of Rochelle Salt. In the following Sections an account is given of the techniques employed in the growing of single crystals of these two substances.

4.2. General.

It is well known that the commonest way to grow crystals is by separation from aqueous solution. This can be accomplished by either of two methods :-

1. Evaporation of a saturated solution.
2. Lowering the temperature of a saturated solution.

Both methods can be used with success but the first method is hardly suitable for a laboratory where fine control is essential. The temperature of a solution can be easily controlled by means of a water-bath and thus the second method lends itself to the production of single crystals.

During the time spent on growing crystals it was found to be axiomatic that the slower the growth the better were the results. The 'growth rate', of course, depends entirely on the rate at which the temperature is lowered so that a good temperature control system is necessary. It was also found necessary to prevent temperature

gradients forming in the crystallising solution as these tended to produce bad effects.

Many attempts were made before reasonably good crystals were obtained and it is thought that crystal growing is more than just the mere application of scientific principles. Approximately nine months were spent in growing crystals - a fact which illustrates the difficulties that can be encountered in this branch of science.

4.3. Production of Single Crystals of Urea.

4.3.1. Growing of Seeds.

As far as could be discovered no large single crystals of Urea had been grown before. Previous workers had only required small crystals (for X-ray purposes etc) which they had obtained quite easily by allowing aqueous or alcoholic solutions to cool. To be of any use in nuclear magnetic resonance experiments the crystals had to be of the order of 1 c.c. in volume. Crystals of this size (and larger) are best grown from small seed crystals set in a saturated solution which is slowly cooled.

First attempts to obtain seed crystals used a rapid

cooling method. Approximately 45 gms. of Analar Urea were dissolved in 40 cc of water at 50°C giving a solution which would be super-saturated at room temperature. The solution was then cooled down rapidly by means of a cold water-bath. Owing to the large solubility factor (see Table 1) the Urea froze out as a mass of closely packed needle-like crystals. Individual crystals could not be separated and their small size would have prohibited their use as seeds.

The above method was repeated with the modification that the solution was cooled down very slowly. This was achieved by placing the beaker containing the solution in a large volume of warm water which was allowed to cool. The crystals obtained by this method were no better than those obtained previously.

The difficulty of obtaining seeds by these methods is best illustrated by the solubility figures given in Table 1 :-

Table 1.

| Temperature (°C) | % solubility | wt. Urea/100gms water |
|---|---|---|
| 20 | 51.9 | 108 |
| 25 | 54.6 | 120 |
| 30 | 57.2 | 134 |
| 35 | 59.8 | 149 |

(contd.)

| Temperature (°C) | % solubility | wt Urea/100 gms water |
|---|---|---|
| 40 | 62.3 | 165 |
| 45 | 64.8 | 184 |
| 50 | 67.2 | 205 |
| 55 | 69.6 | 229 |
| 60 | 71.8 | 254 |

A simple example will, perhaps, clarify the picture:

At 50°C, 100 gm water dissolve 205 gm Urea
and at 30°C, 100 gm water dissolve 134 gm Urea
Therefore, if no water evaporates, a saturated solution at 50°C cooling to 30° C will produce 71 gm Urea from solution for every 100 gm of water present. This relatively large mass of Urea falling from solution accounts for the results obtained by the cooling methods.

The next step in the production of seed crystals was the slow evaporation of a saturated solution at room temperature. The beaker containing the solution was placed in a dark cupboard where it was thought that temperature and humidity variations would be slight. Small crystals were obtained in this manner but still it was difficult to separate individual crystals and again their needle-like shape made them unsuitable for seeds.

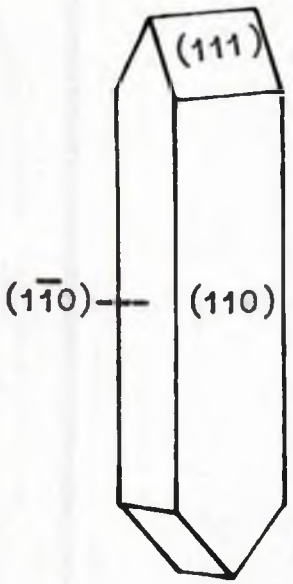


FIGURE 10.

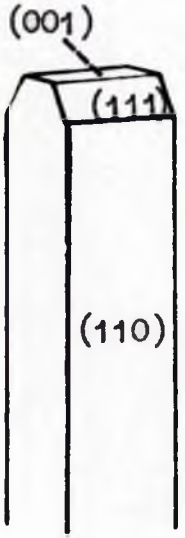


FIGURE 11.

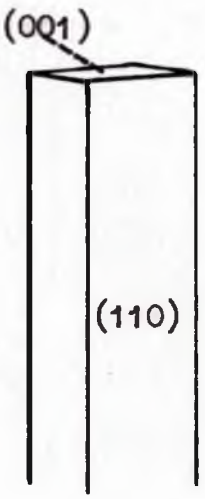


FIGURE 12.

The solution of the problem appeared to lie in the large solubility of the Urea. Other solvents were experimented with and it was found that for methyl alcohol Urea was less soluble by a factor of five than for water. Seeds were obtained from alcoholic solutions of Urea and were of better shape than had ever been obtained. Unfortunately they still suffered from the fault of elongation along one axis. However, the large reduction in the solubility warranted the use of alcoholic solutions in any further experiments.

It is well known that changes in the outward appearance of crystals can be brought about by the deliberate addition of some impurity to the crystallising solution. This is known as 'habit modification' and many examples can be found (see references 27). Bunn (28) found that Urea had an effect on the crystal habit of ammonium chloride and ammonium bromide, and that there was a reciprocal action. The normal habit of Urea grown from alcohol solution is shown in Figure 10. When ammonium chloride, $NH_4Cl$, is present in solution basal planes appear, Figure 11, and when ammonium bromide, $NH_4Br$, is added to the solution the formation of the basal planes obliterates the (111) faces of the Urea crystals completely, Figure 12. These effects result

in a slowing up of thegrowth rate along the c axis i.e. the [001] axis (see Figure 12).

A simple explanation can be given of the above process (28) :

When a face of a crystal of the impurity has a similar structure to a face of the primary crystal, a particle of the impurity will adhere to this crystal face as it would to the corresponding face of its own crystal, since it experiences similar forces. The deposition of impurity on certain crystal faces causes an unstable mixed crystal to be formed on these faces. The fact that the mixed crystal is unstable affords an explanation to the slowing down of the growth rate since the mixed crystal tends to redissolve. From what has been said it would be expected that the greatest modification of habit would result when there was a strong similarity of specific lattice planes, but complete dissimilarity of the rest of the structures. This is borne out by the fact that very small quantities of complex organic substances, such as dyes, cause considerable modification of habit in inorganic crystals.

In the case of ammonium chloride and Urea the (100) plane of ammonium chloride is very similar to the (001) plane of Urea and this is the only pair of planes in which a similarity exists. Therefore strong habit

modification effects should occur. This was, in fact, the case and seed crystals were obtained from an alcoholic solution of Urea plus ammonium chloride. These seeds had lost their needle-like character and the dimensions of a typical seed were 2mm X 2mm X 6mm. Unfortunately the solution had to be almost saturated with respect to ammonium chloride to obtain seeds of suitable dimensions. This was undesirable as ammonium chloride might have been taken up in crystallisation and this would affect the experimental results due to the hydrogen in the ammonium ions.

Ammonium bromide has the same structure as ammonium chloride and the dimensions of the unit cell are such that the similarity between the (100) plane and (001) plane of Urea is greater than in the case of ammonium chloride and Urea. This leads to ammonium bromide having a much stronger effect on the habit of Urea than ammonium chloride. It was found that quite small quantities of ammonium bromide added to alcoholic solutions of Urea gave small seed crystals with a length to width ratio of about three. The majority of these seeds were misshapen and contained flaws but after a number of attempts a few were obtained which were well-shaped and were

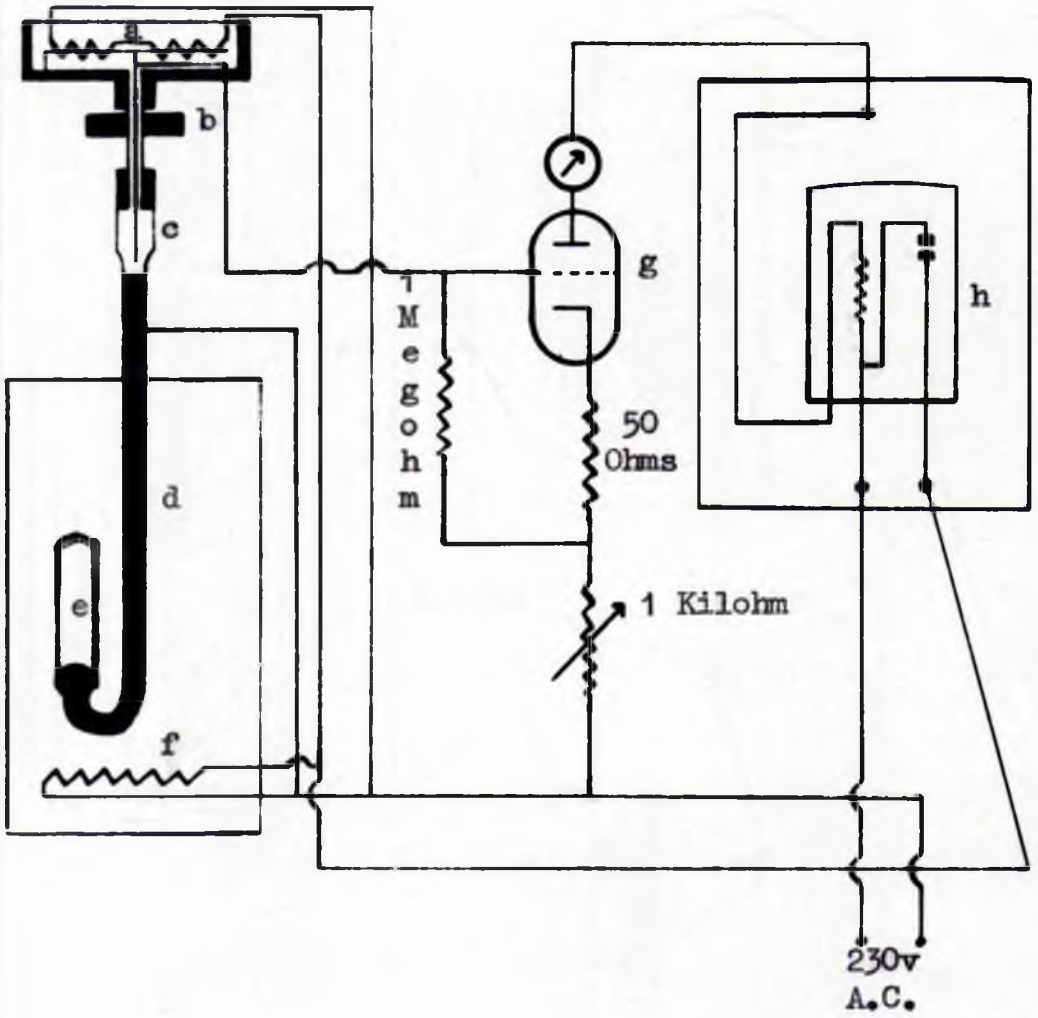


FIGURE 13.

relatively flawless.

4.3.2. Growing of Large Crystals of Urea from Seeds.

Two seeds were drilled and mounted on two small stainless steel pins fixed vertically at the ends of a 3" perspex bar. This bar was fitted with a long stainless steel rod which was attached to a small clock motor so that the bar could be driven at about 15 revs/minute. The bar plus seeds were immersed in a large beaker containing a saturated alcoholic solution of Urea to which a small amount of ammonium bromide had been added. The initial temperature of the solution was 40°C. The beaker, holding approximately a litre of solution, was in turn immersed in a water bath. A cap was fitted to the beaker to prevent excessive evaporation and, in addition, to support the clock motor. The temperature of the water bath was controlled by means of a toluene bulb fitted with a Sunvic Proportioning Head and an electronic circuit. The circuit is shown in Figure 13. and operates as follows:-

Suppose the water-bath heater, f, is on causing a rise in temperature. The toluene, e, will expand pushing the mercury column,d, up until contact is made with the metal needle,c. When this happens the grid of the valve is earthed, the anode current drops and the thermal

vacuum switch,h, opens cutting off the heater. In the Proportioning Head the needle,c, is suspended from a bimetal strip,a, which has a heater in parallel with the bath heater. Therefore, when the switch is closed the bimetal strip expands pushing the needle down towards the rising mercury. When the circuit is open the bimetal strip cools raising the needle out of the mercury and the heaters are switched on again. This process is repeated again and again and the result is that the ordinary 'hunting' experienced with ordinary toluene bulbs is smoothed out due to the superimposition of the rapid variation of the Proportioning Head. With this arrangement a temperature control of $0.01C^{\circ}$ was possible. The position of the needle,c, can be altered by means of an adjusting control, b, so that the temperature can be varied over a range of $2C^{\circ}$. When the needle has reached the end of its travel, mercury can be let in from the reservoir to raise column d and the needle can be reset again.

The temperature of the water-bath was lowered, by means of the above circuit, slowly over the course of a few days - a drop of approximately $3C^{\circ}$ was realised. Two crystals were grown by this means about 3cms.x 0.5cm.x 0.5cm in dimensions. Unfortunately these crystals did not appear to be single but seemed to consist of two or three crystals growing parallel to one another. Trouble was also

experienced with a large number of small crystals forming on the surface of the solution and falling towards the bottom of the beaker. A few of these small crystals fell on the growing crystals and were evident as small seeds protruding from the main crystals. These faults were thought to be the result of too rapid growth and this in turn could be caused by excessive evaporation plus a too sharp temperature drop. It appeared obvious after a few more attempts with this apparatus that a better type of crystal tank would have to be used if good crystals were to be obtained.

A crystal tank was constructed using a Kilner Jar. In normal use this type of vessel has a screw-cap fitted with a rubber ring-seal so that it is completely vapour-tight. A cap was made from paxolin so that the small clock motor could be mounted. This cap used with the ring-seal gave a good vapour-tight tank. Any small leak through the hole in the cap for the driving shaft of the motor was eliminated by fitting a small Gaco ring-seal between the cap and the base of the motor. As this tank was vapour-tight, the vapour above the solution was almost at the temperature of the solution, resulting in an absence of a cold surface in contact with the solution and so reducing the surface crystallisation to a negligible

FIGURE 14.

amount. Alcohol vapour condensed on the relatively cold top surface and walls and streamed back into the solution, thus keeping the walls of the tank washed down. The Kilner Jar and cap are shown in Figure 14.

The water-bath consisted of a perspex tank of dimensions 14" high x 12" x 12". This was filled with water to a level above that of the solution in the crystal tank to ensure a uniformity of temperature in the solution. The bath was heated by a commercial-type heater enclosed in a copper water-tight box situated on the flow of the bath. The temperature of the bath was controlled as described above. A small electric motor drove a propeller in the water-bath at about 100 revs/minute to keep the water in circulation. The level of the bath was maintained constant by adding small amounts of water periodically to make up the loss due to evaporation.

The apparatus described above is the final form of the equipment used in producing single crystals of Urea. Unfortunately, as crystal growing is a continuous process, any fault which develops in the apparatus usually ruins the batch of crystals which is being grown. This was evident several times when power cuts occurred during the night resulting in a relatively rapid cooling of the water-bath which caused the Urea to crystallise out en

masse.

The final crystal growing procedure can be described as follows :-

1. Small seed crystals were obtained from an alcoholic solution of Urea, saturated at room temperature, to which a small amount of ammonium bromide had been added. The best of these seeds were chosen for further growth.

2. 1.5 litres of methyl alcohol saturated with Urea at 45°C were prepared and carefully filtered several times. About 8gms. of ammonium bromide were added to the solution which was transferred(at about 50°C to allow for cooling during transfer) to the crystal tank. The temperature of the water-bath was adjusted to 45°C and then, by adjusting the thermostat control, the temperature was lowered by about ¼C° per day until the temperature of the bath had reached 40°C. During this time Urea crystals had formed on the foot of the tank and had been left to grow undisturbed. Two seed crystals were then drilled and placed on the stainless steel pins of the crystal rotator. Before immersion in the crystal tank, the seeds were dipped in warm alcohol to remove any surface impurities and to create fresh surfaces to facilitate growth.

3. After the seeds were placed in position, the cap of

the crystal tank was screwed down to prevent evaporation and the rotation of the crystals was then started.

4. By means of the thermostat control the temperature of the bath as lowered by approximately $\frac{1}{4}C^{o}$ per day for about two weeks. The seed crystals grew quite well although several attempts were required before suitable crystals were obtained (mainly due to circumstances outwith the author's control e.g. power cuts, heater failure.)

5. To remove the crystals from the tank, the clock motor was stopped although the thermostat was kept running and the cap of the tank was withdrawn until the crystals were in the vapour above the alcoholic solution. They were allowed to remain there until they had cooled down then they were withdrawn slightly further and cooled again. When it was deemed that the crystals had cooled sufficiently to prevent them cracking they were removed from their supports.

Only two suitable crystals were grown by the above method and this fact illustrates the great difficulty in growing single crystals of Urea. The smaller of the two crystals weighed approximately 1.0gm. and had dimensions 2·5 cm. x 0·6 cm. x 0·5 cm. The other crystal, which had the better shape, weighed 1·6gm. and had dimensions

2·9 cm. x 0·7 cm. x 0·6 cm. These crystals were of an ideal size and shape for nuclear magnetic resonance work and therefore no attempt was made to produce larger specimens. The crystals had to be stored in a desiccator as Urea is slightly deliquescent.

4.3.3. Conclusion.

The main point of note in the growing of single crystals of Urea is that the growth rate must be very slow. Unless this condition is met the crystals tend to become compound and their external appearance is very indefinite. This was the reason for allowing crystals to form on the foot of the crystal tank, For a given drop in temperature the growth rate per crystal is inversely proportional to the number of growing crystals so that, in this way, the rate at which the seed crystals developed was very slow indeed.

The two good crystals were examined under a polarising microscope and were found to be quite singular in character. In order to discover if any appreciable amount of ammonium bromide had been taken up in crystallisation, some of the crystals which had been growing on the foot of the tank were dissolved in ammonia-free water and the solution was tested with Nessler's reagent. This test showed that there was no detectable amount of ammonium

ion present. It was therefore safe to conclude that, at least for experimental requirements, the crystals were pure Urea.

One final point worth noting is the rotation of the crystals while growing. This serves two purposes :-

1. Fresh solution is continually being presented to the crystal faces

2. Temperature gradients are prevented from forming in the solution by the stirring action of the crystal support; the design of the support was such that the solution and crystals did not rotate continuously together.

4.4. Production of Single Crystals of Rochelle Salt.

Rochelle Salt is very similar to Urea in that it is very soluble in water. Fortunately, however, in contrast to Urea, it is quite easy to crystallise and , in fact, Rochelle Salt crystals are grown on a commercial basis.

The technique employed here was basically the same as that used for Urea; seed crystals were placed in a saturated solution and the temperature was slowly lowered. The main difference between the two methods was in the simplicity of the crystal tank used for growing the Rochelle Salt crystals. This consisted of a large beaker

with a thin layer of paraffin placed on top of the crystallising solution to prevent evaporation.

Seed crystals were prepared as before by allowing a saturated solution to evaporate slowly. An aqueous solution of Rochelle Salt saturated at 40°C was prepared. This solution was heated to about 50°C (to avoid precipitation) and then carefully filtered into the crystal tank. The thermostat was set so that the temperature of the bath was about ½° above the saturation point and the seed crystals were placed in position; the seeds were suspended by hairs from a rod placed across the top of the tank, two seeds being in the tank at the one time. The thin layer of paraffin (previously warmed to 40°C) was then added to the solution. Initially the rate of cooling was 0.1° per day but after two days this was increased to about 0.3° per day. This method is a slight modification of the technique used by Moore (29). After the crystals had reached suitable dimensions, they were removed from the bath and washed with alcohol to remove any trace of paraffin.

Several crystals were grown by this means. The weights and sizes of these crystals were quite varied although the growth of some was controlled to enable them to be used in experiments without having to be cut.


FIGURE 15.

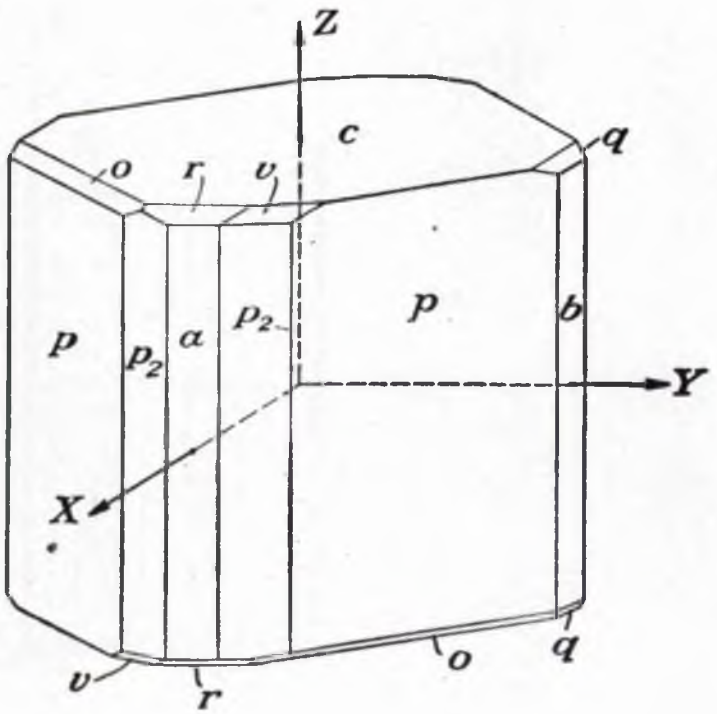


FIGURE 16.

Figure 15 shows a typical crystal grown by this method. The weight of this crystal was about 29gms. and its dimensions were as follows :-

| | |
|---|---|
| Length along x-axis | 2·2cms |
| Length along y-axis | 3·3cms |
| Length along z-axis | 3·7cms |

This crystal was flawless and was so perfectly shaped that it was possible to determine the crystal axes from ordinary contact goniometer measurements.

Figure 16 is taken from Cady (30) and shows an idealised Rochelle Salt crystal. Comparison of the prepared specimen with this figure enabled the various faces to be identified and referring to the results given below it is clearly seen that the agreement between the observed inter-facial angles and the values given by Cady is excellent.

Table 2.

| Inter-facial angle | Cady (Fig.16) | Observed |
|---|---|---|
| $\angle a p_1$ | 22°35' | 22°30' ± 30' |
| $\angle a p$ | 39°43' | 40°0' ± 30' |
| $\angle a b$ | 90° | 90°0' ± 30' |
| $\angle b.c$ | 90° | 90°0' ± 30' |

Thus, by these simple measurements, were the directions of the crystal axes determined uniquely.

Since Rochelle Salt contains water of crystallisation,

it has a vapour pressure and this prevents the storage of these crystals in desiccators. If the humidity of the atmosphere is less than 37% at room temperature (20°C) then the crystal loses water and dehydrates. Above 88% humidity the crystal absorbs water and becomes deliquescent. Fortunately the atmospheric conditions experienced in this laboratory are such that the relative humidity at room temperature lies in the range 45% - 70% (figures based on student experiments, supervised by author, in this laboratory over the course of 3 years). Consequently these crystals lay unprotected for two years and no loss of transparency or sign of deliquescence was noticed during this period.

The conclusion drawn from this work was that Rochelle Salt is fairly easily grown in the form of single crystals. Care must be taken not to warm the crystallising solution above 55°C since at this temperature Rochelle Salt breaks up into sodium tartrate and potassium tartrate and the process is irreversible.

4.5. Discussion.

The production of large clear crystals of extremely soluble substances is not at all simple. It is difficult to lay down any set of hard and fast rules as each substance seems to require its own special technique.

However, one point worth stressing again is that of

slow growth. Slow growth means greater opportunities for the atoms, ions or molecules to pack together to form a good crystal. It is also helpful, when growing crystals to a specific size, to choose a suitable impurity to add to the solution so that the habit of the crystal can be modified to suit the requirements.

In all it may be said that crystal growing is more of an art than a science.

# SECTION 5.

# 5. UREA.

## 5.1. Introduction.

As shown in Section 2. the study of the proton magnetic resonance absorption spectrum of a crystal containing hydrogen atoms can sometimes enable the positions of the protons to be located in the unit cell of the crystal lattice. Some idea, however, of the basic elements of the crystal structure must be known. Therefore it can be said that this type of work complements that of X-ray and electron diffraction which can provide accurate cell co-ordinates for the heavier atoms, but which can only give a very rough indication of the positions of hydrogen atoms. Moreover, the magnetic properties of the hydrogen nucleus are such that a good signal strength is obtained and thus fairly reliable results can be produced. The limitations of the method are such that only fairly simple crystal structures can be investigated otherwise the theoretical interpretation of the results becomes extremely difficult.

The interest in Urea, $OC(NH_2)_2$, was partly historical. It was one of the first organic substances to be synthesized and, on account of its simple structure, it was one of the first materials to be studied by X-ray crystallographers (31).

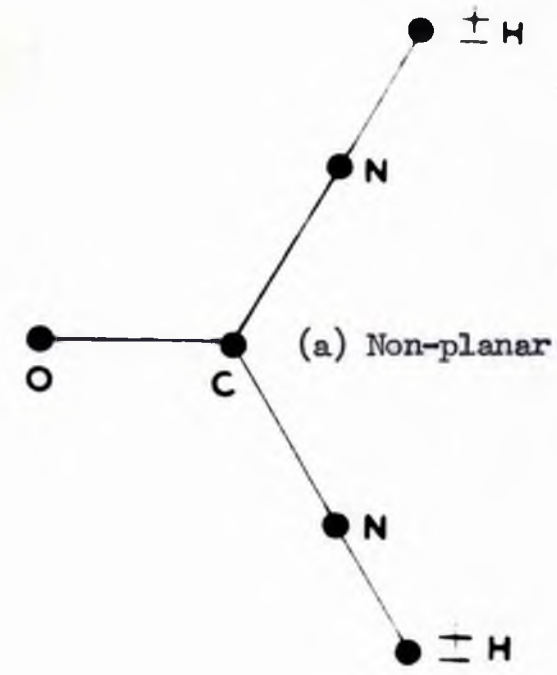


(a) Non-planar

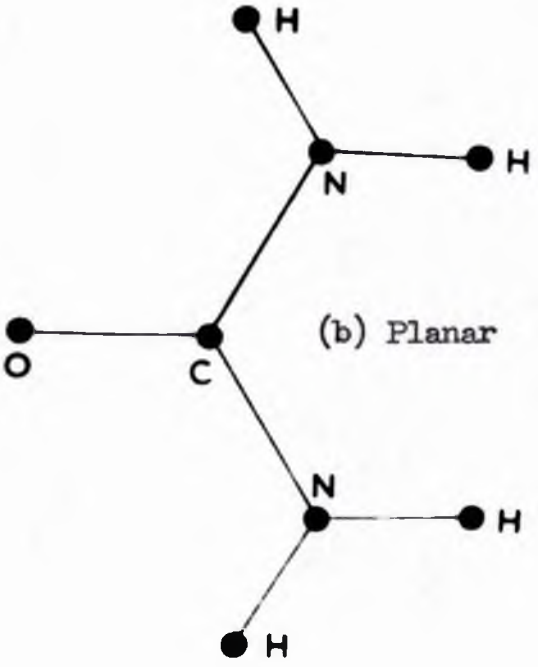


(b) Planar

FIGURE 17.

In addition, the only other magnetic nucleus present, other than the proton, is $N^{14}$; $C^{12}$ and $O^{16}$ both have zero spin (and thus no magnetic moment) and contribute nothing to the width of the absorption line. This fact makes the interpretation of the experimental data much simpler.

It is known from X-ray analysis that the four heavy atoms of the Urea molecule lie in a plane (32,33,34,35, 36) and the arrangement has $C_{2v}$ symmetry. It has not been clear, however, whether the four hydrogen atoms lie in the same plane as the heavy atoms, or whether they lie symmetrically above and below this plane, or whether the overall configuration has lower symmetry than $C_{2v}$. In any previous work on Urea two models for the molecular structure have been put forward. Kellner (37) assumed the symmetrical non-planar model shown in Figure 17(a) where the hydrogen atoms are symmetrically disposed above and below the plane containing the heavier atoms and, on this basis, analysed her infra-red spectra. On the other hand, later analyses of infra-red spectroscopic measurements on monocrystalline Urea (38,39) have suggested that the whole molecule is planar as indicated in Figure 17(b). This model is supported by the X-ray work of Vaughan and Donohue (36) who suggest positions

for the hydrogen atoms which they deduced from their diffraction patterns. Therefore, it seemed that Urea would provide an excellent example where nuclear magnetic resonance could distinguish between two rival structures and perhaps provide some quantitative information concerning the positions of the protons.

In the following Sections it is shown that by a study of the variation with orientation of the mean square width (second moment) of the absorption spectrum the non-planar model of the Urea molecule is incorrect, and that within experimental error the molecule is plane with symmetry $C_{2v}$. Finally, values are given to the molecular parameters associated with the $NH_2$ group.

5.2. Molecular and Crystal Structure.

Urea, $OC(NH_2)_2$, crystallises in tetragonal form and the dimensions of the unit cell are (36)

$$a = b = 5.661A^{\circ} \qquad c = 4.712A^{\circ}$$

These figures, together with the specific gravity of 1.335, show that two molecules of Urea are contained in the unit cell. The cell parameters of the heavy atoms are given by

$$C \text{ at } 0, \tfrac{1}{2}, z_c ; \tfrac{1}{2}, 0, \bar{z}_c$$

$$O \text{ at } 0, \tfrac{1}{2}, z_o ; \tfrac{1}{2}, 0, \bar{z}_o$$

$$N \text{ at } x_N, \tfrac{1}{2}-x_N, z_N ; \tfrac{1}{2}-x_N, \bar{x}_N, \bar{z}_N ;$$
$$\bar{x}_N, x_N+\tfrac{1}{2}, z_N ; x_N+\tfrac{1}{2}, x_N, \bar{z}_N$$

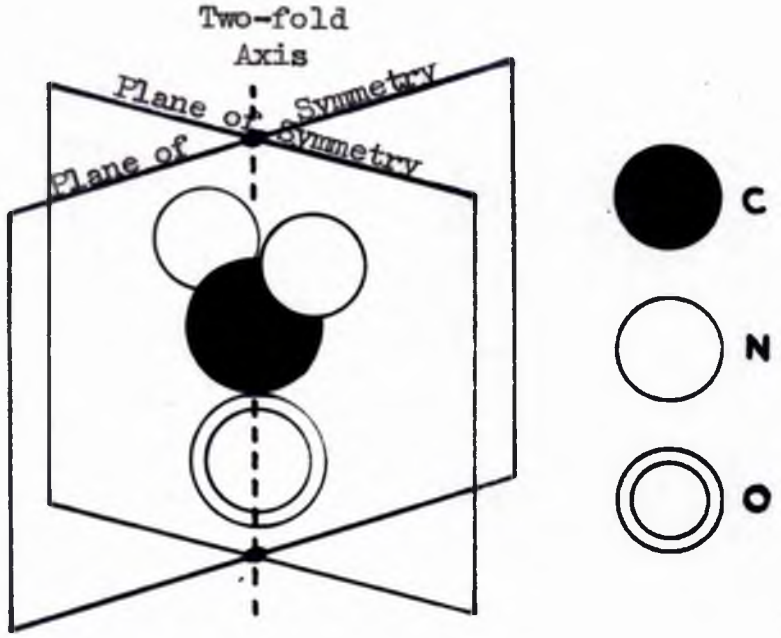


FIGURE 18.

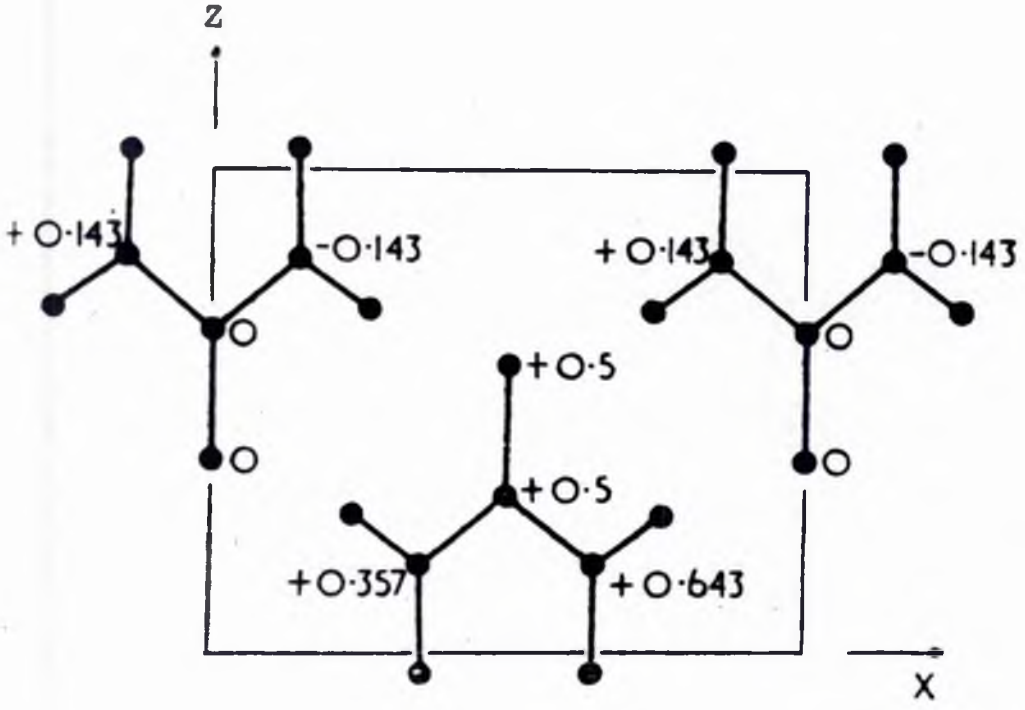


FIGURE 19.

where $Z_c = 0.3308$ $Z_o = 0.5987$

$X_n = 0.1429$ $Z_n = 0.1848$

As stated previously the heavy atoms of the Urea molecule all lie in a plane; the molecule itself has two planes of symmetry and one twofold axis of symmetry (see Figure 18). The tetragonal unit cell is shown in Figure 19, a projection on the xz plane being depicted (the numbers alongside the atoms are their fractional y co-ordinates); the planes of the molecules all include the Z direction and are inclined alternately at 45° and 135° to the plane of the diagram thus the planes of alternate molecules lie parallel to the (110) and $(1\bar{1}0)$ planes respectively i.e. along the diagonal planes of the unit cell. From Figure 18 it is clearly seen that the arrangement of heavy atoms has symmetry $C_{2v}$ and if either of the two models proposed is correct this symmetry will not change owing to the symmetrical disposition of the hydrogen atoms.

The interatomic distances and angles used in this work were those given by Vaughan and Donohue and are given below

$O - C = 1.262A^{\circ}$ $C - N = 1.335A^{\circ}$

$\hat{OCN} = 121^{\circ}$ $\hat{NCN} = 118^{\circ}$

## 5.3. Experimental Procedure.

### 5.3.1. Use of rectangular r-f coils.

In the Appendix to the paper by Bloembergen et alia (9) it is shown that the signal to noise ratio obtained from any nuclear magnetic resonance experiment is dependent on a large number of circuit variables. One such parameter is the so-called 'filling factor' of the coil. This quantity can be defined as that fraction of the total r-f energy that is actually stored in the space occupied by the sample.

If ordinary circular coils were used then, owing to the rectangular cross-section of the Urea crystals, it was found that the filling factor was $\sim 0.6$. Obviously the best result would be got with a crystal of square cross-section when this factor would be $\sim 0{\cdot}64$. It was thus thought that approximately a 50% increase in signal to noise ratio would be obtained by using rectangular coils so shaped to fit snugly round the crystal. This was quite an important point since preliminary experiments had shown that Urea gave a broad absorption line and a poor signal to noise ratio.

The rectangular coils were constructed from 18 s.w.g. copper wire which was first softened by heat and then wound on brass formers having the same cross-section as

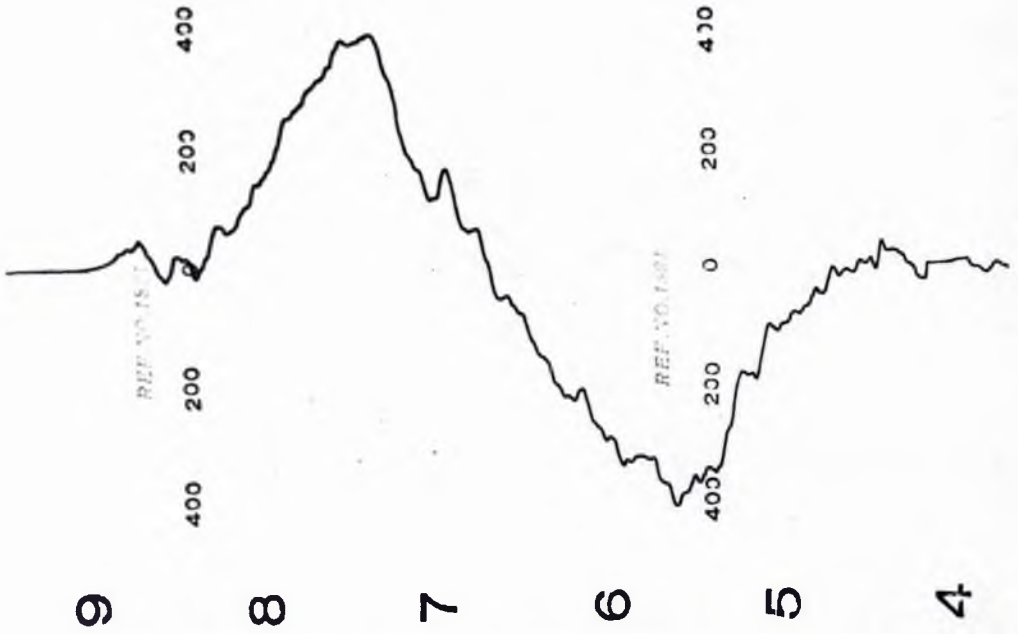


Trace obtained using circular coil.

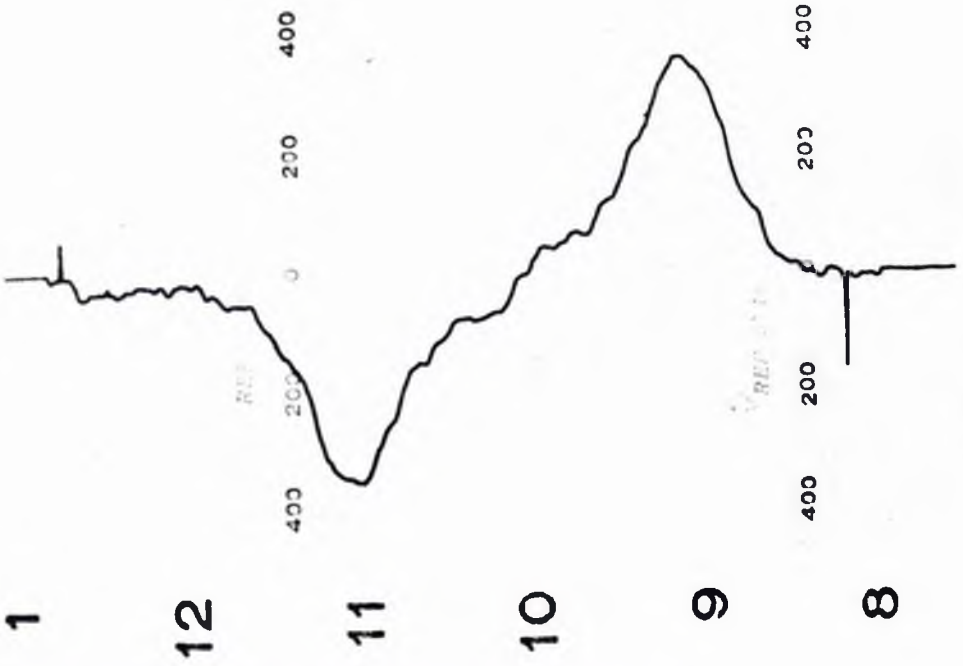


Trace obtained using rectangular coil.

FIGURE 20.

the respective crystals. The two coils thus made each had a Q-factor of about 140 and the filling factor was increased to ~ 0·9. The improvement obtained is shown in Figure 20 where experimental traces using circular and rectangular coils are compared.

5.3.2. Measurement of Experimental Second Moment.

In order to obtain accurate results in work of this nature it is necessary to carry out measurements at a low enough temperature to suppress any molecular motion which might affect the width of the resonance spectrum i.e. in order to justify the assuption of a rigid lattice. Experiments were performed as a sample of polycrystalline Urea at room temperature and at 90°K; no significant difference in the second moment of the absorption lines was detected and thus it was assumed that at room temperature the lattice was effectively rigid. It can, however, be mentioned here that owing to the relatively poor signal to noise ratio obtained from this powder sample there was some uncertainty in the results and if there was any change in the value of the second moment then it lay within the experimental error and therefore was not apparent. Accordingly it was assumed that the lattice was rigid and all future measurements were performed at room temperature.

Owing to the nature of the signal arising from Urea and since permanent records were required, the lock-in amplifier system was used for studying the spectrum. As stated previously the output from the lock-in amplifier is proportional to the slope of the absorption line and is fed into a recording microammeter. This meter, therefore, traces out the first derivative of the absorption line(see Fig.20) and, for a normal curve, if the line width is defined as the interval in gauss between maximum and minimum slope then it can be found directly from the derivative curve by measuring directly the interval between the maximum and minimum peaks. In this type of measurement the amplitude of the modulating field must not be too great to obscure any fine structure which the line might contain and yet it must be large enough to give a reasonable signal to noise ratio. Preliminary experiments were carried out to determine the best operating conditions and in the final measurements a peak-to-peak modulation amplitude of 3 gauss was used (this was $< \frac{1}{4}$ of the line width and thus a faithful reproduction of the first derivative was still obtained). Each derivative plot was accurately calibrated in terms of gauss by means of the calibration pips seen on each side of the trace (Fig.20).

The second moments can be obtained directly from the

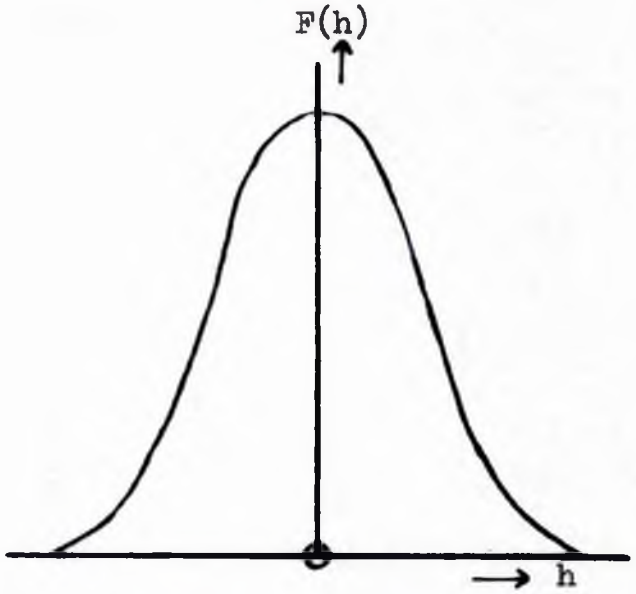


Absorption curve

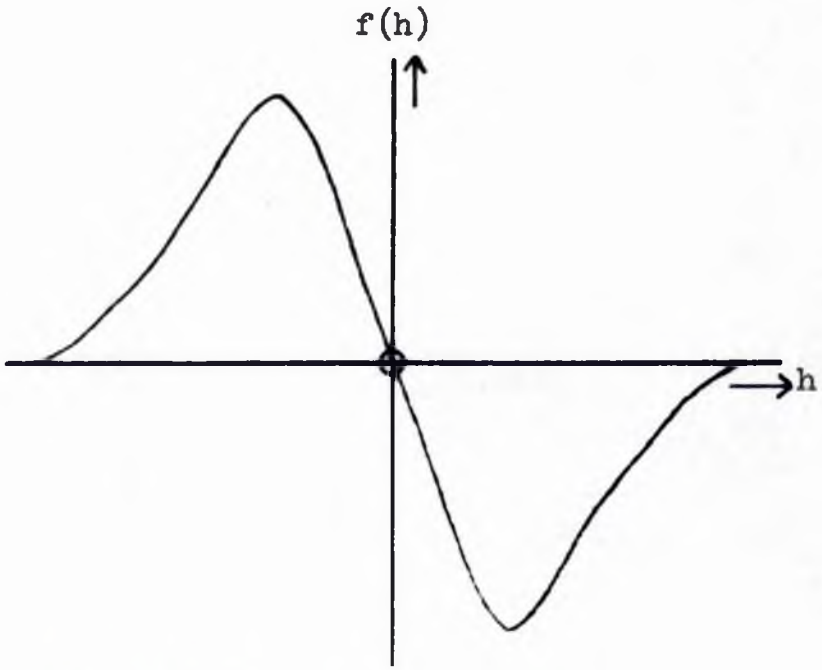


Derivative of absorption curve

FIGURE 21.

experimental traces. Consider a normal absorption curve and its derivative (Figure 21). It can be shown that the second moment of the absorption line is given by

$$S = \frac{\int_{-\infty}^{\infty} \mathcal{L}^2 F(\mathcal{L})\, d\mathcal{L}}{\int_{-\infty}^{\infty} F(\mathcal{L})\, d\mathcal{L}} \qquad (5.1.)$$

where $F(\mathcal{L})$ is the height of the absorption curve at field H and $\mathcal{L} = H - H_o$, $H_o$ being the resonant field value. The denominator must be introduced to normalise $F(\mathcal{L})$ (see Section 2.3.). This expression can be rewritten in terms of $dF(\mathcal{L}) / d\mathcal{L} = f(\mathcal{L})$, which is indicated by the output of the lock-in amplifier, giving

$$S = \frac{1}{3} \frac{\int_{-\infty}^{\infty} \mathcal{L}^3 f(\mathcal{L})\, d\mathcal{L}}{\int_{-\infty}^{\infty} \mathcal{L} f(\mathcal{L})\, d\mathcal{L}} \qquad (5.2.)$$

$\mathcal{L}$, $f(\mathcal{L})$ are found directly from the experimental plots and the integrals are evaluated using the trapezium rule so that the final expression is

$$S = \frac{\Sigma \mathcal{L}^3 f(\mathcal{L})}{3 \Sigma \mathcal{L} f(\mathcal{L})} \qquad (5.3.)$$

This expression was used during the course of this work to evaluate all the experimental second moments.

As the immediate problem was the diferentiation between two proposed models as against accurate structure determination it was decided that the initial experiments should be performed on the smaller of the two available crystals. This crystal was placed in its appropriate coil and then mounted with its tetrad [001] axis along

the vertical axis of rotation, and perpendicular to the steady magnetic field $H_o$. The resonance spectrum derivative was then recorded, at $5^o$ intervals, for values of $\phi_o$ between $0^o$ and $180^o$, $\phi_o$ being the azimuth angle of the field measured from the [100] direction. Several runs were made at each setting of the crystal and the second moment of each spectrum was calculated, the mean for each setting being taken. The crystal was then mounted with its [110] axis perpendicular to the field, and the polar angle $\gamma_o$ of the field (measured from the [001] direction) was varied by rotation of the crystal about this axis. As the crystal was long in its tetragonal direction it was necessary to cut the crystal into four pieces and stack them in the coil. The cutting of the crystal was performed by a wet-thread technique :

The blade was removed from a small hacksaw and replaced by a strong thread with a large enough tension on it to ensure an accurate cut. A small brass cutting guide was constructed into which the crystal fitted quite securely. Two vertical slits were let into the sides of the guide to prevent the cutting thread from wandering. The thread of the saw was kept continually damp (but not too wet) and it was found that by this means it was possible to make a cut of about $\frac{1}{2}$sq.cm. in 15 mins. Care was taken not to let surplus water attack the crystal and it was found

advantageous to line the foot of the guide with a strip of blotting paper. With care quite reasonable cuts were made and no great loss in filling factor resulted from the cutting and stacking. Fortunately the shape of the coil tended to align the pieces and it was thought that any error arising from lack of parallelism would be within the final experimental error. With this new crystal mounting, the resonance spectrum was again recorded, at $5^{\circ}$ intervals for values of $\psi_0$ between $0^{\circ}$ and $180^{\circ}$. Several runs were taken at each setting and the second moment calculated in each case, the mean being taken. The results obtained from this crystal will be given in a later Section when they will be compared with data arising from theoretical considerations of the structure of Urea. This work has been briefly reported (40) and was sufficient to support the entirely planar model of the molecule.

When it was shown that the non-planar model was incorrect the obvious step was to obtain more accurate experimental results in order to put the planar model on a more quantitative basis. The experiments were thus repeated using the larger crystal. The increase in crystal size resulted in a noticeable increase in signal to noise ratio which in turn meant a reduction in the experimental uncertainty of the second moment calculations. A typical

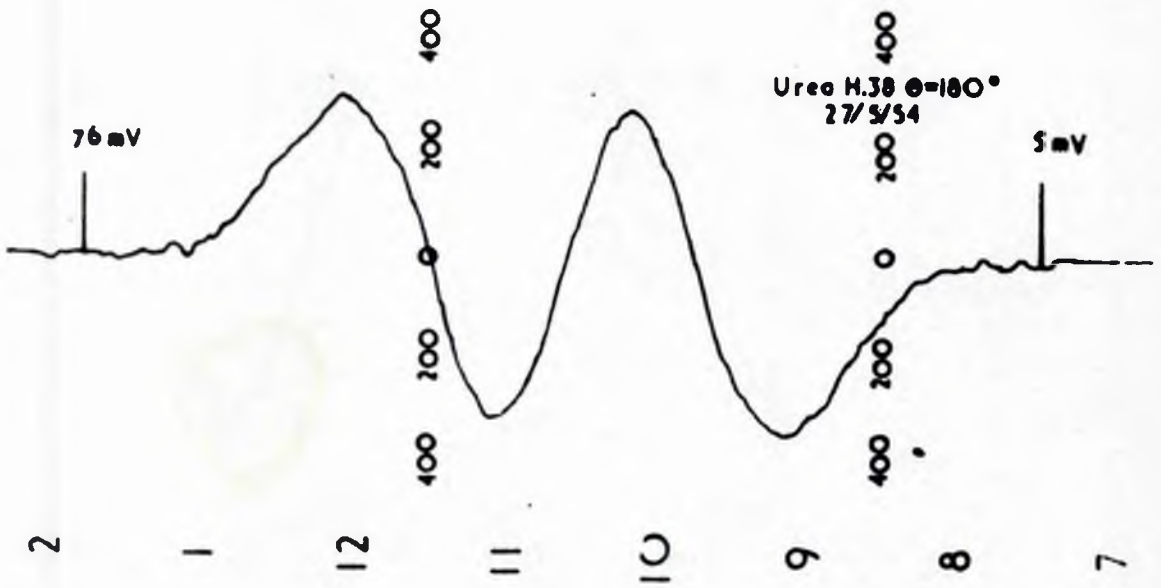


FIGURE 22A.

record is shown in Figure 22A. This trace illustrates the reduction in noise when compared with Figure 20 and it also shows the variation in line shape with orientation. This 'fine structure' was used as a check on the final results and will be discussed later.

Perlman and Bloom (41) have shown that there is a broadening effect of the observed spectrum due to the finite amplitude of the modulating field and this introduces an appreciable error in the second moment calculations. Andrew (42) made a direct calculation of the effect and showed that the true second moment S is related to the observed second moment S' by the expression

$$S' = S + \tfrac{1}{4} h_m^2 \qquad (5.4)$$

where $h_m$ is the amplitude of the field modulation. With the amplitude of 1.5 gauss used in the above experiments this meant that the true second moments were obtained by subtracting 0.6 $gauss^2$ from all the observed values. This correction was only applied in the case of the results obtained from the second set of experiments.

After the experimental results had been calculated for the second crystal it was found that there was a large discrepancy between the values obtained for rotation about the [001] axis and the corresponding values from the first crystal. As the results for rotation about

the tetrad axis agreed this pointed to some error incurred in the cutting and stacking of the second crystal in the r-f coil. On removal of the pieces of the crystal from the coil it was found that one portion had inadvertently been rotated through $90^\circ$ and so accounted for the difference in results. However, by knowing the fraction of the crystal which had been misplaced it was possible to convert the results obtained into values corresponding to what would have been obtained if the crystal had been properly stacked. This was done as follows:-

Let $f(\theta)$ be the second moment corresponding to correct stacking at some angle $\theta$ to the applied field

Let $F(\theta)$ be the observed second moment due to a fraction $(1 - \alpha)$ of the crystal rotated through $90^\circ$

Then

$$F(\theta) = \alpha f(\theta) + (1-\alpha) f(\theta + 90^\circ)$$

$$F(\theta + 90^\circ) = \alpha f(\theta + 90^\circ) + (1-\alpha) f(\theta)$$

from which the expression for $f(\theta)$ is

$$f(\theta) = \frac{\alpha F(\theta) - (1-\alpha) F(\theta + 90^\circ)}{2\alpha - 1}$$

By weighing the various pieces of crystal it was found that $\alpha = 0{\cdot}74$. A smooth graph of $F(\theta)$ against $\theta$ was then drawn from which values of $F(\theta + 90^\circ)$ could be obtained. The values of $f(\theta)$ from $0^\circ$ to $180^\circ$ were then calculated

and the results obtained agreed with the initial experiments performed on the first crystal. However, it was thought advisable to repeat all the experiments again with the correct crystal stacking. This was done and the results obtained were those used in the final calculation of the positions of the protons in the Urea molecule.

5.4. Interpretation of Results.

In order to differentiate between the two molecular structures it was necessary to compare the observed anisotropy of the second moment with theoretical results based on each model. Theoretical values of the second moment were calculated for both planar and non-planar structures using Eq.(2.12) given in Section 2.3. As initially only a qualitative picture was required certain approximations were used in the calculations. The second term in Eq.(2.12) was neglected as it was shown that the contribution to the second moment from the nitrogen nuclei would amount to only 5%. This expression therefore reduced to

$$S = \frac{44\gamma\cdot4}{N_R} \sum (3\cos^2\theta_{jk} - 1)^2 r_{jk}^{-6} \qquad (5.5)$$

where $r_{jk}$ is given in Angstrom units. Before proceeding further it will perhaps be advantageous if the various parameters of the above equation are considered in some detail. $\theta_{jk}$ is the angle between the inter-nuclear vector $r_{jk}$ and the applied magnetic field $H_0$ and since

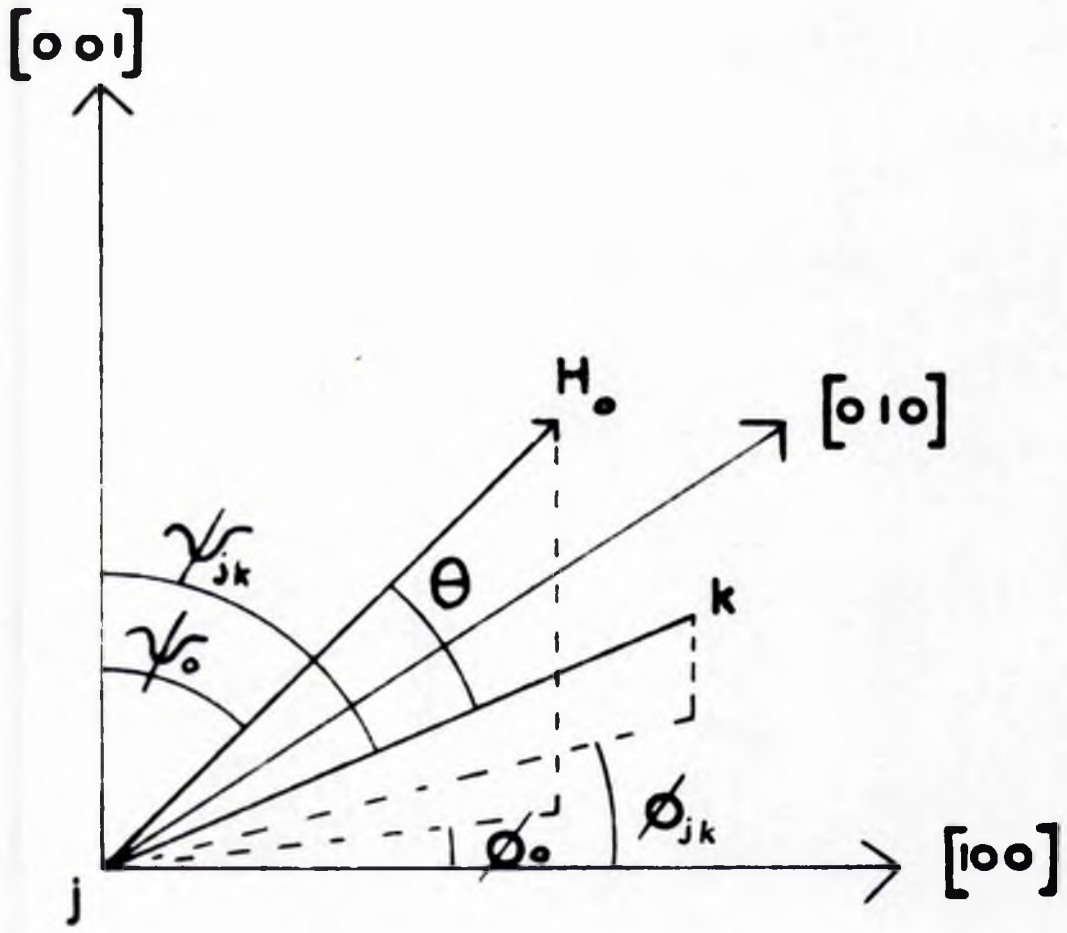


FIGURE 22.

the angles varied in the experiments were measured between $H_o$ and the crystal axes some correlation is necessary. From Figure 22, where $\psi_{jk}$ is the polar angle and $\phi_{jk}$ the azimuthal angle of $r_{jk}$, $\psi_o$ is the polar angle and $\phi_o$ the azimuthal angle of $H_o$ referred to the crystal axes as shown, it follows that

$$\cos\theta_{jk} = \cos\psi_o \cos\psi_{jk} + \sin\psi_o \sin\psi_{jk} \cos(\phi_{jk} - \phi_o) \qquad (5.6)$$

Therefore in calculating $(3\cos^2\theta_{jk} - 1)r_{jk}^{-6}$ it is necessary to describe each vector $r_{jk}$ in terms of its length, polar angle and azimuthal angle.

Normally the expression for the second moment is split into an intra-molecular part and an inter-molecular part. However, in this case it did not simplify the situation and thus, in Eq.(5.5.), $N_k$ refers to the sample as a whole. Fortunately, the molecular and crystal symmetry of either model are such that there are only a few typical protons, the rest being equivalent to some respective one of these few. It can be shown (Appendix 1) that there are 8 typical protons in Urea - 4 corresponding to the molecules in planes parallel to (110) and 4 from the molecules in planes parallel to $(1\bar{1}0)$.

To assist in the calculation of the second moments a model of the unit cell of Urea was constructed. A photograph of this model is given in Figure 23. and shows

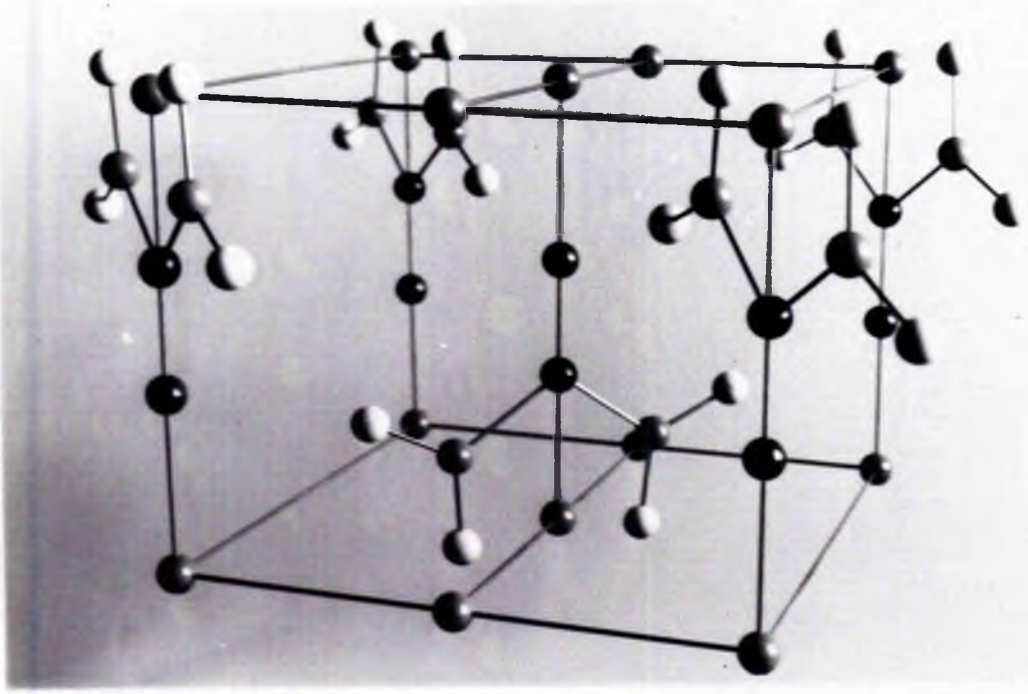

(a) Planar Model.

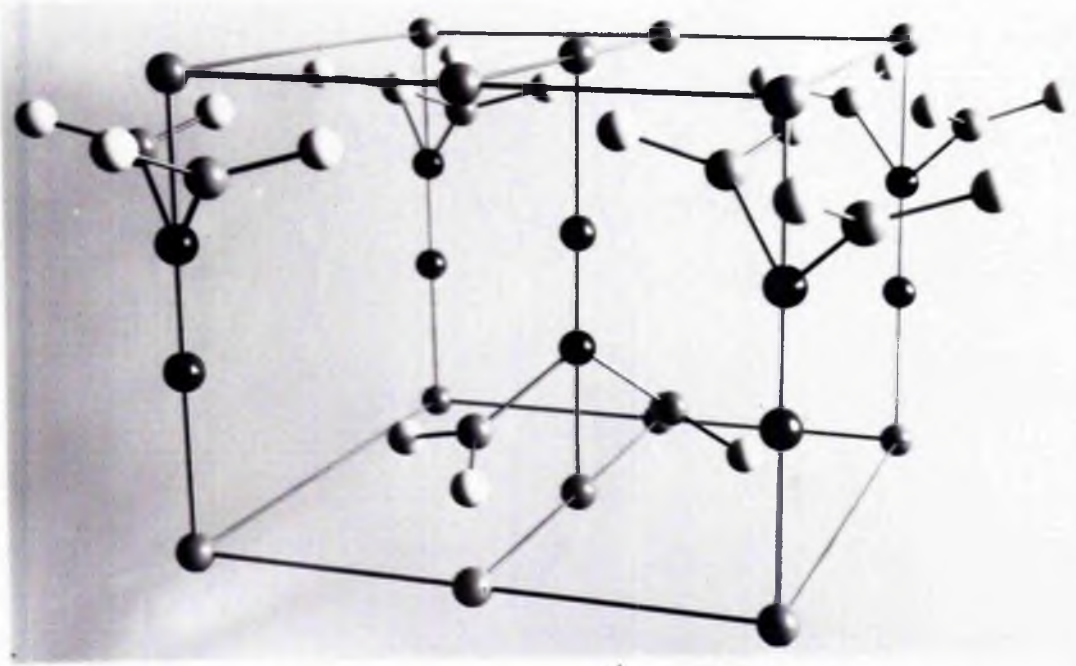

(b) Non-planar Model.

FIGURE 23.

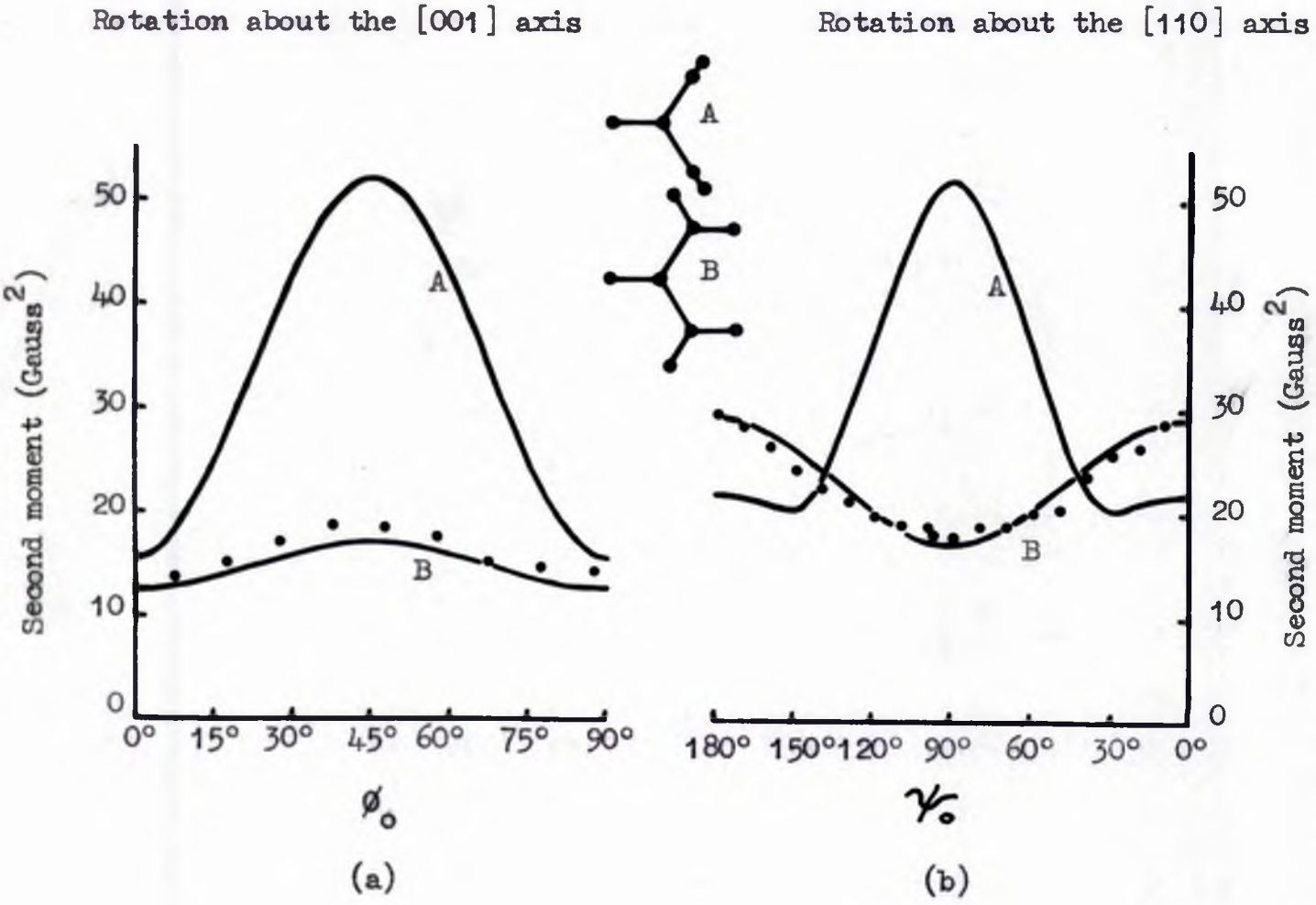
Rotation about the [001] axis
Rotation about the [110] axis
A
B
Second moment (Gauss$^2$)
50
40
30
20
10
0
0° 15° 30° 45° 60° 75° 90°
$\phi_0$
180° 150° 120° 90° 60° 30° 0°
$\gamma_0$
(a)
(b)

FIGURE 24.

(a) the planar model, (b) the non-planar model. The initial results are shown in Figure 24. (curves A for the non-planar structure, curves B for the planar structure) where the behaviour of the theoretical second moment is compared with the experimental results. Results are only given for one quadrant of the fourfold symmetrical pattern in (a) and for half of the twofold symmetrical pattern in (b). The positions in the unit cell of the O, C and N atoms, as determined by Vaughan and Donohue (36), were used in the theoretical calculations. The length of the N-H bond was taken as $1{\cdot}00A^{\circ}$, and the C-N-H angle as $120^{\circ}$ in both planar and non-planar models. In the case of the non-planar structure it was also assumed that the plane defined by each $NH_2$ group included the carbon atom of the molecule. Any small deviation from this last assumption would lead to only small changes in curves A since the form of variation of the second moment is mainly determined by the contribution of the proton pairs of the $NH_2$ groups. In the actual calculations neighbours up to a distance of $3A^{\circ}$ were treated exactly according to Eq.(5.5), while the contribution of the more distant nuclei was obtained by assuming that they were evenly distributed from $3A^{\circ}$ to infinity and applying the formula for a powder where there is no angular dependence. This gave a contribution of $3{\cdot}0$ gauss$^2$ to the second moment which represented a

contribution to the total varying from 10% - 20% in the individual cases.

A study of the curves in Figure 24 shows that there is good agreement between theory and experiment for the planar model but no agreement in the case of the non-planar model; indeed, for rotation about the [110] axis even the qualitative form of variation is different. These results were therefore sufficient to determine the planar structure of the Urea molecule and it was thought that, even with the assumptions and approximations made, the assumed parameters would not be out by more than 10%.

Since it had been shown that the non-planar model was incorrect, attention was focussed on the experimental results obtained from the larger crystal. These results were more accurate due to improved signal to noise ratio and were all corrected for the modulation broadening effect; the broadening effect due to the inhomogeneity of the permanent magnet was small enough to be neglected. Careful analysis of the results showed that the probable experimental error was $0 \cdot 3$ gauss$^2$. This was small enough to enable an accurate determination of the molecular parameters to be carried out. Several trial calculations showed that, in order to obtain good agreement between theory and experiment only the three extreme values of the curves (See Figs.24,26)

needed to be compared with the corresponding experimental results. These results were more accurately determined than the others and if agreement with theory was obtained for them then it was found that all intermediate experimental and theoretical values were in quite good agreement.

In calculating the theoretical second moments the nitrogen contribution was not neglected and detailed calculations were made of interactions up to 5A$^{o}$ using the formula

$$S = \frac{447.4}{N_R} \sum (3\cos^2\theta_{jk} - 1)^2 r_{jk}^{-6} + \frac{2.774}{N_R} \sum (3\cos^2\theta_{jf} - 1)^2 r_{jf}^{-6} + 0.6 \text{ gauss}^2 \qquad (5.7)$$

where the symbols are defined as in Section 2.3. and the third term is due to protons beyond 5A$^{o}$. This type of calculation involved the consideration of 27 unit cells and the interactions of an $NH_2$ group with its 46 nearest neighbours. Beyond 5A$^{o}$ the protons were assumed to be evenly distributed and the powder formula was applied; the contribution to the second moment was approximately 2% and any variation with orientation would be negligible.

In order to determine accurately the positions of the

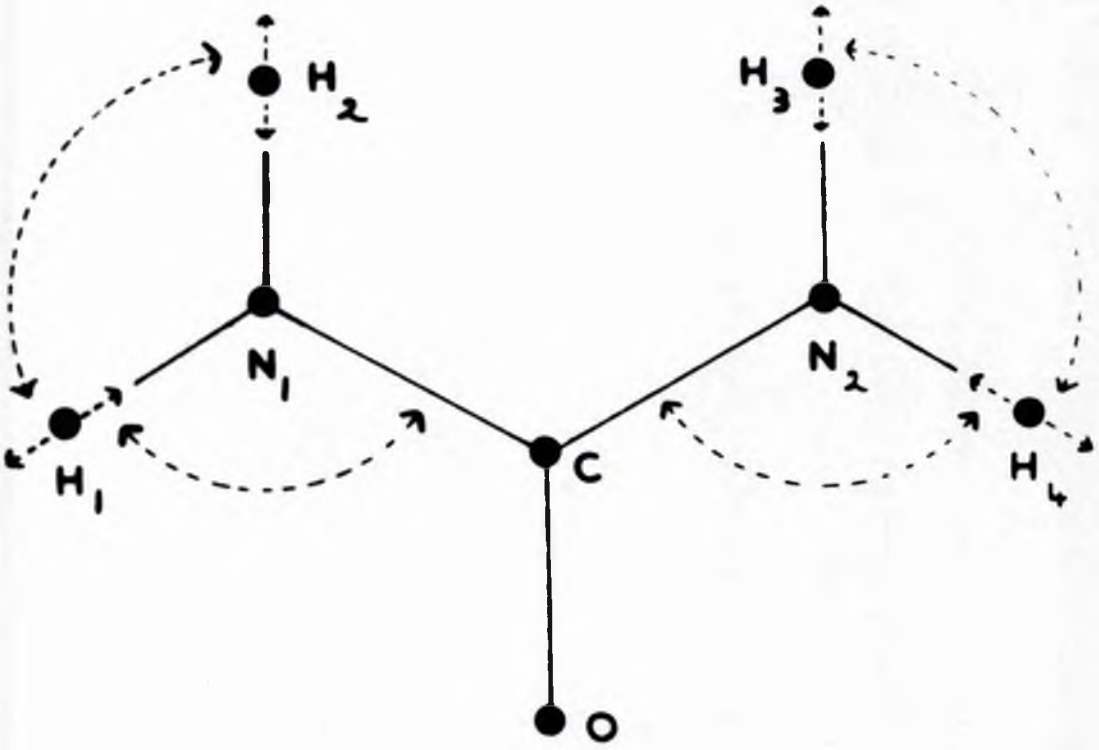


FIGURE 25.

hydrogen atoms relative to the known structure of the O, C and N atoms shown in Figure 25, four parameters are needed:

(a) The bond length $N_1$-$H_1$

(b) The bond length $N_1$-$H_2$

(c) The angle $H_1N_1H_2$

(d) The angle $CN_1H_1$.

Since only three experimental results are available only three theoretical parameters can be determined uniquely. Therefore, to reduce the number of variables, it was assumed that the bonds $N_1$-$H_1$ and $N_1$-$H_2$ were equal. This assumption was justified on the strength that there was no evidence to suggest that this should not be the case. Values of this bond length along with the two angles mentioned above were then sought to bring agreement between the theoretical and experimental results.

A number of molecular models were proposed and the theoretical second moments were calculated for the three extreme values. These values corresponded to the following orientations of the crystal:-

1. $H_o$ along the [100] axis i.e. $\psi_o = 90^o$, $\phi_o = 0^o$
2. $H_o$ along the [110] axis i.e. $\psi_o = 90^o$, $\phi_o = 45^o$
3. $H_o$ along the [001] axis i.e. $\psi_o = 0^o$ , $\phi_o = 45^o$

A list of the models used and the results obtained is given in Appendix 2. A study of the trial models showed that reasonable agreement with experiment resulted if the N-H bonds were taken to be $1{\cdot}04A^o$ and the angles as $120^o$

each. The sum of the squares of the differences between the three theoretical and experimental pairs of second moments was used as a measure of disagreement. With this close agreement it was now possible to obtain perfect correlation between theory and experiment. A small change was made in each of the three molecular parameters separately, and the second moment calculated in each case. These results are given in Table 3. along with the mean experimental results for the three orientations. The second moment values were then written as a function of the three variables and expanded by Taylor's theorem. Finally to obtain perfect agreement between theory and experiment it remained to solve three linear equations in three variables.

Table 3.

| | | | Values of Second moment(gauss$^2$) | | |
|---|---|---|---|---|---|
| N-H bond | $H_1\hat{N}_1H_2$ | $C\hat{N}_1H_1$ | $H_o$ along [100] | $H_o$ along [110] | $H_o$ along [001] |
| 1·04 | 120° | 120° | 13·5 | 18·6 | 29·3 |
| 1·02 | 120° | 120° | 13·9 | 19·6 | 31·8 |
| 1·04 | 122° | 120° | 12·9 | 19·2 | 27·2 |
| 1·04 | 120° | 118° | 13·8 | 17·8 | 31·8 |
| Mean experimental values | | | 13·6 | 18·2 | 29·0 |

Rotation about the [001] axis

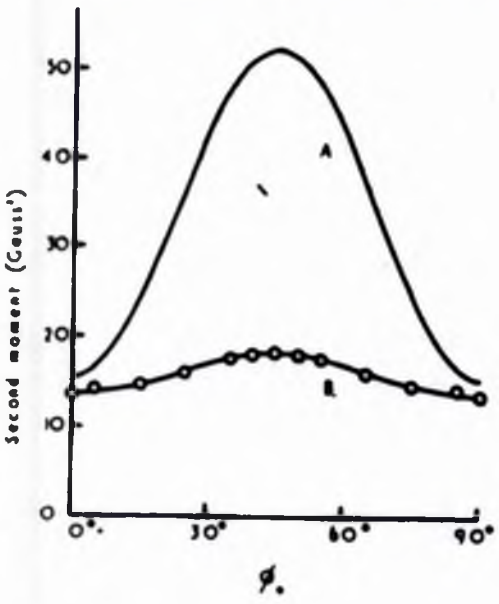


(a)

Rotation about the [110] axis

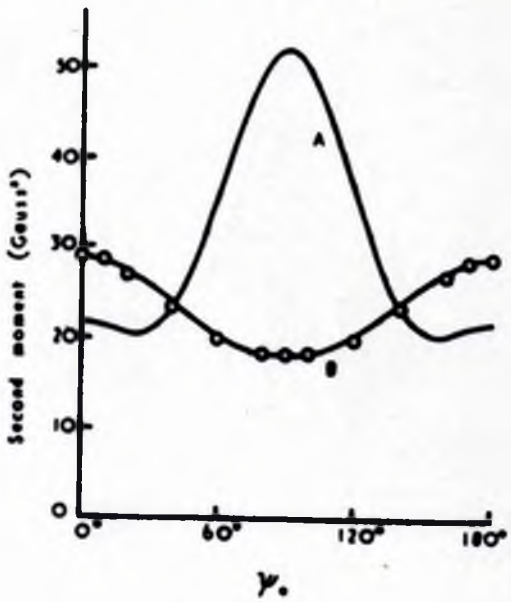


(b)

FIGURE 26.

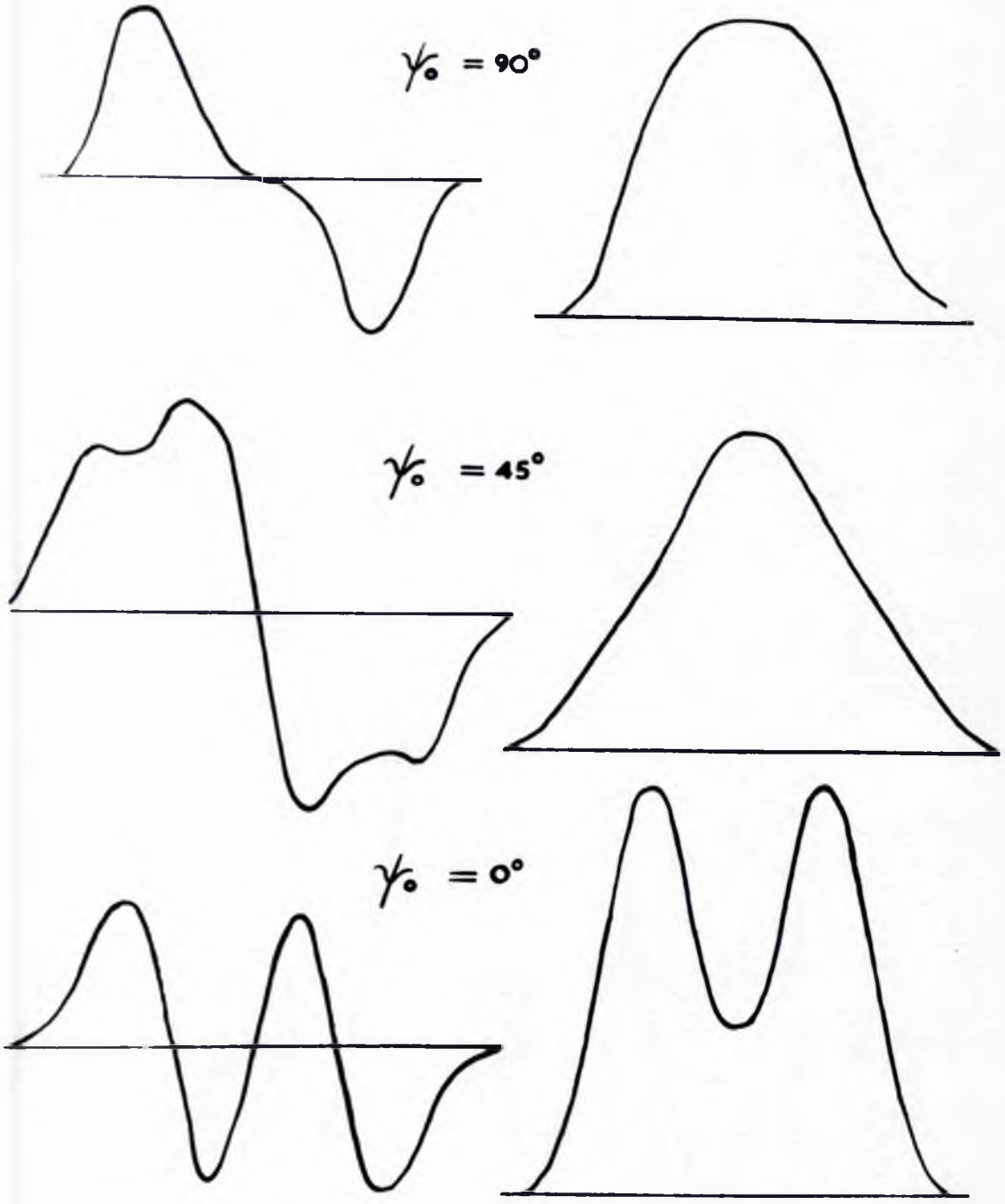


FIGURE 27.

A detailed account of the method is given in Appendix 3. The values of the three molecular parameters given by this calculation were as follows :

N-H bond length of 1·046A°

$H_1N_1H_2$ bond angle of 119·1°

$CN_1H_1$ bond angle of 120·5°

Using the estimated experimental error of ± 0·3 gauss[2] the accuracy of the bond length was found to be ± 0·01 A°, and of the angles ± 2°. A simple calculation gave the proton-proton separation in each $NH_2$ group as 1·80 ±0·02A°.

The final results are shown in Figure 26 where the theoretical curves based on the above molecular parameters. It can be seen from the graphs that the consideration of only the extreme values was justified as the intermediate points do in fact fall into line with theory.

5.5. Measurement of fine structure.

For rotation about the [110] axis it was found that, in general, the absorption line derivatives contained fine structure. Figure 27 shows three representative experimental plots with their integrals; these integrals are, of course, the absorption lines corresponding to the respective orientations. As can be seen the fine structure was most pronounced when $H_o$ was parallel to the [001] direction i.e. $\psi_o = 0$, $\phi_o = 45°$; the absorption line had the characteristic double hump obtained from a system of

proton pairs (1). Referring to Figure 25, when $H_o$ is parallel to the [001] direction i.e. parallel to the C-O bonds, the proton pairs in the $NH_2$ groups are orientated with the same angle $\theta$ with respect to the field. This holds for both types of molecule in the unit cell and therefore, to a first approximation, the Urea crystal can be regarded as a two-proton system with broadening effects due to nearest neighbours.

In Section 2.2 the separation of the two resonance lines obtained from a two-proton system is given as

$$2\alpha(3\cos^2\theta - 1)$$

$$\text{where } \alpha = \tfrac{3}{2}\mu r^{-3}$$

Putting $r = 1{\cdot}80 \pm 0{\cdot}02A^{\circ}$ and $\theta = 31 \pm 1{\cdot}5^{\circ}$ (obtained from final second moment calculations) into the above equation gives the result that the separation of the two lines should be $8{\cdot}7 \pm 0{\cdot}5$ gauss. This is for the planar model and $H_o$ parallel to the tetragonal axis. The mean value of the line separation obtained from the experimental traces (or integrated plots) was $8{\cdot}9 \pm 0{\cdot}2$ gauss. This additional information lends further support to the molecular parameters obtained from the second moment data. If, however, the non-planar model of the molecule had been correct, then all the proton-proton vectors would have been perpendicular to $H_o$ for the above orientation, and the separation of the two lines would have been only 7·2 gauss for a proton-proton distance of $1{\cdot}80A^{\circ}$.

To obtain agreement for this model the above inter-nuclear distance would have to be reduced to 1·68A°.

Again the experimental results show that the planar structure of the Urea molecule is the correct one and some quantitative confirmation of the assumed molecular parameters is obtained.

5.6. Discussion and Future Research.

The length of the N-H bond i.e. 1·046A° found in Urea is longer than in general. A careful study of results published for other substances reveals that the length of this bond usually lies in the range 1·03 ± 0·02A°. For example, the bond length in ammonia is 1·014A°(43) and it ranges from 1·03 to 1·035A° for the ammonium halides (44, 45, 46). This increase in bond length can probably be explained by the presence of hydrogen bonds which are thought to exist in Urea. Richards and co-workers found that hydrogen bonding to oxygen did result in an increase in the N-H bond in certain hydrazine salts. They found an N-H bond length of 1·048A° and that in hydrazine fluoride, where very strong hydrogen bonds occur, the bond was increased to 1·075A° (47, 48). Therefore it appears that the structure proposed for the Urea molecule is quite feasible. However, it is possible that some other model would fit the experimental results and then it would be

impossible to distinguish the correct structure by the above methods.

All the work reported herein has been based on two major assumptions :

1. The N-H bonds are equal
2. The lattice is rigid at room temperature.

However, there is some unpublished evidence which suggests that these assumptions may be slightly incorrect. Firstly, with reference to the N-H bonds, Levy (49), from a neutron diffraction study of Urea, reports unequal N-H bond lengths. His model for the Urea molecule is

$N_1H_1 = 1{\cdot}04A^{\circ}$ $\qquad$ $N_1H_2 = 0{\cdot}98A^{\circ}$

$H_1\hat{N}_1H_2 = 119^{\circ}$ $\qquad$ $C\hat{N}_1H_1 = 121^{\circ}$

This model does not give agreement with experiment in nuclear magnetic resonance work as can be seen from Appendix 2. Secondly, some work on powdered Urea suggests that there is some form of internal motion occurring in Urea at room temperature (50). If this is correct then the results given here would have to be modified slightly. Even so, assuming the bond angles correct (cf. values given by Levy), there is reason to suppose that the N-H bond lengths would only be reduced by a few per cent.

In order to ascertain whether or not molecular motion

is occurring it is proposed in the immediate future to examine carefully the absorption spectrum of a single crystal of Urea with varying temperature.
Obviously at room temperature the narrowing effect of any motion present must have been small enough to remain undetected in the initial experiments on Urea powder. It has been stated, however, that the experimental uncertainty in the measured second moment was fairly large due to the poor signal to noise ratio arising from the powder sample. This, of course, would enable any small reduction in second moment to be overlooked. With the advent of the accurate results obtained from the single crystal it will be possible to ascertain at what temperature the molecular motion, if any, sets in and thus the experiments can be repeated at some temperature where it is certain that the lattice is effectively rigid. This will enable a new molecular model to be proposed but, as mentioned above, the previous results should not be affected by more than a few per cent.

Summarising, the research reported here illustrates the value of nuclear magnetic resonance in determining the positions of protons in simple crystal structures, the main features of which are already known. In particular, the planar structure of the Urea molecule has been shown to be correct

and some idea of the parameters in the amino groups has been obtained.

A full account of this work has been given (51).

# SECTION 6.

# 6. Rochelle Salt

## 6.1. Introduction.

The interest in Rochelle Salt lay in its ferroelectric properties and the existing hydrogen-bond theory which has been put forward to explain the unusual dielectric anomaly occurring in this salt.

Rochelle Salt (sodium potassium tartrate tetrahydrate) has the chemical formula Na $KC_4H_4O_6 \cdot 4H_2O$ and has crystal symmetry $D_2$. However, in the range - 18°C to 24°C there is a slight change from orthorhombic symmetry to monoclinic and the crystal has ferroelectric properties i.e. spontaneous polarisation occurs in the $\pm$ x direction. In this temperature range the dielectric constant along the X-axis shows an anomalous behaviour although it is normal along the y and z axes at all temperatures. With analogy to ferromagnetism these characteristic temperatures are called the Curie temperatures.

As the theory of ferroelectricity in Rochelle Salt appears to be incomplete it will be advisable to review briefly the various proposed explanations and show how nuclear magnetic resonance could perhaps shed some light on the existing theories. In view of the complicated crystal structure, however, only qualitative information could be hoped for from this technique.

## 6.2. Review of Ferroelectric Theories.

With the analogy to ferromagnetism Fowler (52) attempted to develop a Langevin-Weiss type of theory using a model in which the $H_2O$ molecules formed rotating dipoles. This theory, however, was deficient in that it ignored piezoelectric interaction and since the crystal structure had not been determined a direct calculation of the dipole interactions was not possible. These considerations coupled with the fact that there was no independent evidence of movable dipoles led to the abandonment of this explanation.

Mueller (53) in a series of papers developed his so-called 'interaction theory' which took into account the piezoelectric properties of Rochelle Salt. This was quite successful and gave quite a reasonable account of the observed physical properties but unfortunately it gave no explanation of the mechanism involved.

With the determination by Beevers and Hughes(54) of the structure of Rochelle Salt, coupled with the discovery of ferroelectricity in KDP, attention was turned to the properties of the hydrogen bonds existing in both these substances. Mason(55) proposed a theory based on the movement of hydrogen nuclei along the hydrogen bonds. Since the bonds in question exist between water molecules and oxygen ions he assumed them to be asymmetric. By calculating the probability involved of a hydrogen nucleus

moving between two potential wells of different depths he obtained an expression for the dielectric constant which agreed quite well with experiment. These bonds were also discussed by Ubbelohde and Woodward (56). Unfortunately there are several objections to this model which can be enumerated as follows:-

1. Two independent mechanisms are postulated to explain the two Curie temperatures.

2. The theory predicts a large entropy change at the upper Curie temperature and therefore a large specific heat anomaly should occur. This contradicts experiment where the anomaly is found to be very small.

3. Substitution of deuterium for hydrogen results in only slight changes in the dielectric behaviour whereas substitution of a few per cent of potassium by rubidium causes the dielectric anomaly to disappear. This can be contrasted with the case of KDP where the Curie temperature is raised considerably by the replacement of hydrogen with deuterium.

4. Mathias (57) compared Rochelle Salt with lithium ammonium tartrate ($LiNH_4C_4O_6H_2O$) which is also ferroelectric. He found that the value of the spontaneous polarisation in each case was the same although this new tartrate contained only one molecule of water of crystallisation as opposed to the four in Rochelle Salt. He suggested that the water molecules played a relatively unimportant part in the ferroelectric

behaviour.

5. From a neutron diffraction study of Rochelle Salt Pepinsky (58) suggests that structural changes do take place in the ferroelectric range but that these are not only confined to the hydrogen bonds. He also states that preliminary work shows that the hydrogen bond used by Mason to explain the ferroelectric properties, viz. the $O_{1,10}$ bond (see Reference 55), will not prove significant. It will be interesting to see what results a more detailed study by this method gives.

6. Megaw (59), in a review paper, suggests that the anomalous behaviour might be due to motion of the potassium ions as opposed to motion of hydrogen nuclei.

With these facts in mind it was thought worth while to make a nuclear magnetic resonance study of Rochelle Salt to test this existing hydrogen-bond theory. Since this theory involves the movement of hydrogen atoms it might be expected that the proton line width would show a narrowing on entering the ferroelectric region. It could also be hoped that if this theory was correct then a relaxation time study might lead to a value of the height of the potential barrier separating the two potential wells.

Both line shapes and relaxation times have been measured for powdered and single crystal samples from 170°K to 315°K. In addition an investigation of the effect on the above

quantities of electric fields imposed on the single crystal sample was measured.

6.3. Experimental Procedure.

6.3.1. Measurement of Line Shapes.

All the absorption line derivatives were recorded as described previously using a modulation amplitude small in comparison to the breadth of the line. Runs were carried out over the temperature range 170°K-315°K for both powder and single crystal samples, the temperature being controlled by the gas-flow system described in Section 3.4.

The powdered samples were compressed into small glass cylinders which fitted snugly inside the r-f coil; the compression produced a better signal to noise ratio due to increased filling factor.

No attempt was made to shape the single crystal used in these experiments. It was approximately 3·0 cms long and was roughly diamond-shaped in cross-section, the diagonals measuring approximately 1·7 cms and 2·0 cms. As in the case of Urea, the r-f coil was wound directly on to the crystal to ensure a good filling factor. The derivatives were all recorded with $\underline{H}_o$ directed along the x-axis of the crystal (deduced from goniometric measurements). In addition, the effect of an electric field on the line width at room temperature was noted. Fields of 500 v/cm A.C. and 500 v/cm D.C were obtained by means of a condenser arrangement situated in the gap of the magnet, the direction of the electric field

being along the x-axis in all cases.

Experimental values of the line-width were obtained from the recorded derivatives and line-width vs. temperature curves are shown in Figures 28, 30 for the powder and single crystal respectively.

6.3.2. Measurement of Relaxation Times.

Since preliminary experiments showed that the relaxation time at the lowest temperature was of the order of 10 sec. an indirect method of measurement was used throughout the temperature range. The technique employed is that given by Bloembergen et alia (9). This method is based on Eqn. (2.18) and assumes that a given degree of saturation is associated with the same value of $\gamma^2 H_1^2 T_1 T_2$ when $\omega_m T_1 >> 1$, $\omega_m$ being the modulation angular frequency. Therefore when $\gamma^2 H_1^2 T_1 T_2 = 1$ i.e. at half intensity of absorption,

$$(H_1^2 T_1 T_2)_x = (H_1^2 T_1 T_2)_y \qquad (6.1.)$$

where x and y denote two values of the temperature. The ratio $(T_2)_x / (T_2)_y$ can be obtained from the inverse ratio of the line-widths at the two temperatures (see Section 2.4.), and $H_1$ is proportional to the signal generator output. Thus it is possible to obtain relative values of $T_1$ over the range of temperature in terms of the relaxation time at the lowest temperature. Absolute values of $T_1$ could be obtained if it were possible to measure the relaxation time directly at the lowest

temperature by some other method. Unfortunately in the case of Rochelle Salt this was not possible as $T_1$ was too short at the lowest working temperature. However, a method was devised which at least gave a rough value to $T_1$.

It will be seen that from the expression

$$\gamma^2 H_1^2 T_1 T_2 = 1 \qquad (6.2.)$$

a knowledge of $H_1$ and $T_2$ would determine $T_1$. Now for a Gaussian shape function the ratio of the total line width to the line width, as defined here, is 3.6. Several line shapes were plotted for benzene using the same r-f coil as for Rochelle Salt. From the derivative curves obtained it was found that the above ratio had a mean value of 3.4. Therefore it was assumed that the proton magnetic resonance line from benzene had a Gaussian shape at 247°K (the temperature at which the experiments were carried out). For this shape of curve the expression

$$\frac{1}{T_2} = (2\pi)^{-\frac{1}{2}} \gamma \Delta H \qquad (6.3.)$$

holds, where the symbols have their usual significance, and so it was possible to calculate $T_2$ for the benzene sample. From Reference (11) the value of $T_1$ for benzene at 247°K was found. Finally, by performing a saturation curve relaxation time measurement (as described above) and using $\gamma^2 H_1^2 T_1 T_2 = 1$ it was possible to find the factor of proportionality between $H_1$ and the signal generator output for the given r-f coil.

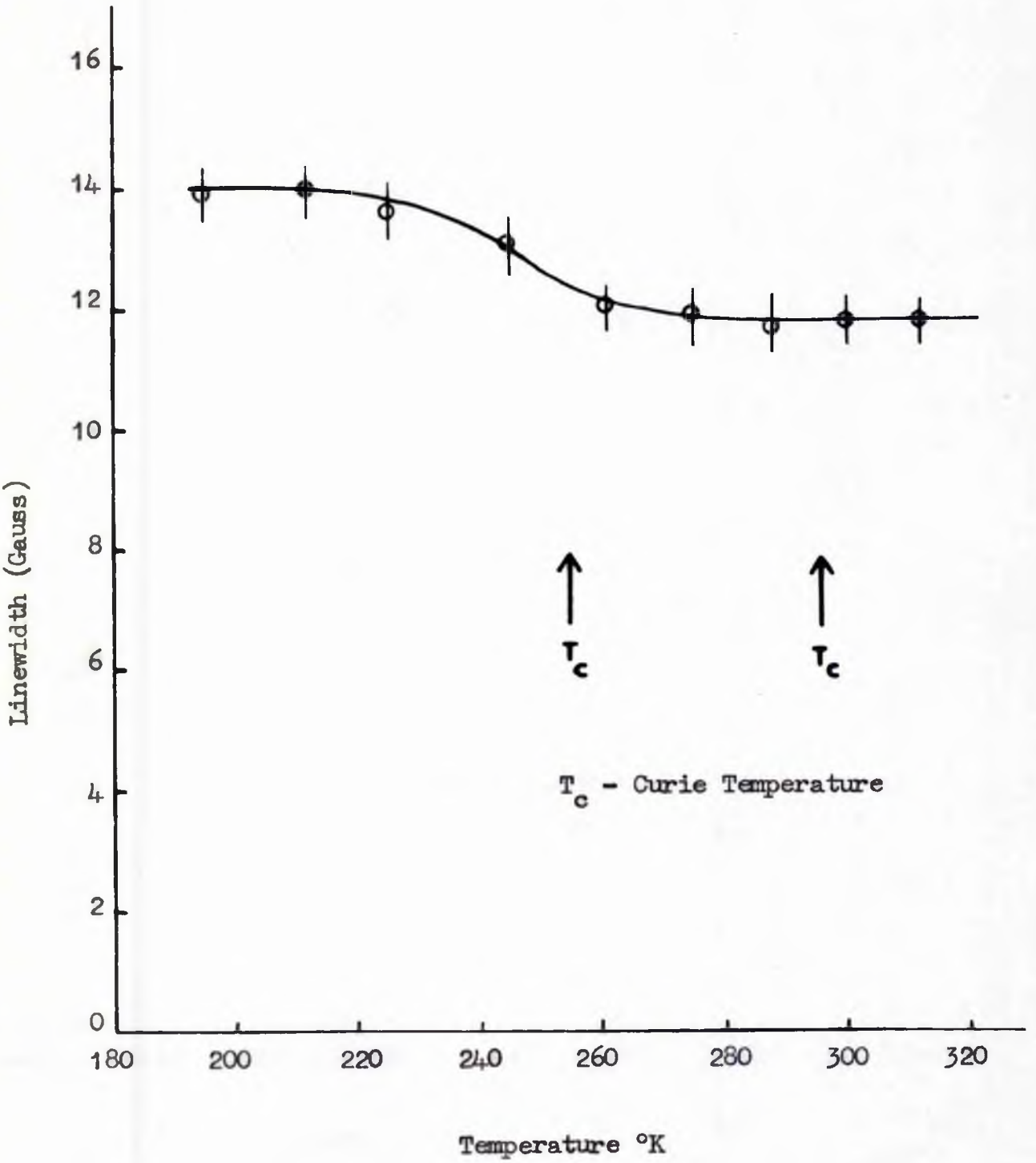
16
14
12
10
8
6
4
2
0
Linewidth (Gauss)
180
200
220
240
260
280
300
320
Temperature °K
$T_c$
$T_c$
$T_c$ - Curie Temperature

FIGURE 28.

From a study of the line shapes of the Rochelle Salt powder between 170°K and 315°K it was found that the total line width to line width ratio varied between 2.0 and 2.9. In spite of this the line shape was taken as Gaussian and $T_2$ calculated at 190°K using Eqn. (6.3.). This value of $T_2$ was a mean value over the temperature range 170°K - 210°K since the line width did not change obviously over this range. From the experimental data and substituting for $H_1$, $T_2$, $\gamma$ in Eqn. (6.2.) the value of $T_1$ at 190°K was calculated for Rochelle Salt. The value for $T_1$ at this temperature was found by this method to be 8 sec. This compares favourably with the initial observations that the relaxation time at low temperatures was of the order of 10 sec. No great accuracy is claimed for this method as the assumption that all lines are of Gaussian form is very approximate. However, it appears to give the correct order although the actual value probably has an error of $\pm$ 30%. Fortunately the interest lies in relative values of the relaxation times rather than their absolute values. Figures 29, 31 show the relaxation time measurements for the powder and single crystal respectively.

As in the line width experiments the effect on the relaxation time produced by an electric field was noted in the case of the single crystal.

## 6.4. Discussion of Results

### 6.4.1. Powder Sample

The line-width vs. temperature curve is shown in Figure 28.

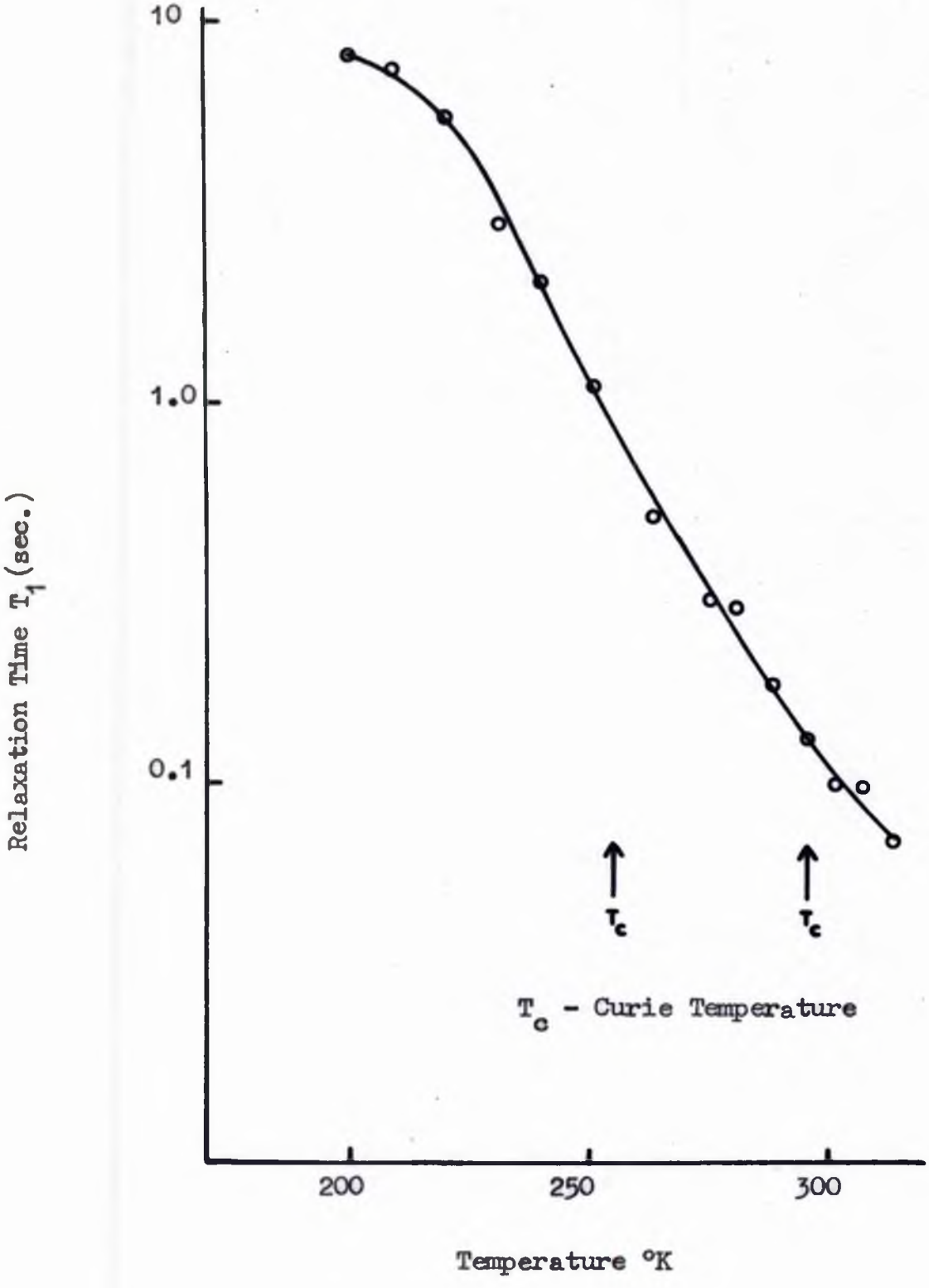
10
1.0
0.1
Relaxation Time $T_1$ (sec.)
$T_c$
$T_c$
$T_c$ - Curie Temperature
200
250
300
Temperature °K

FIGURE 29.

Owing to the poor signal to noise ratio resulting from the use of a powder sample there was an appreciable experimental uncertainty in the determination of the line-widths. This error is represented by the vertical lines at the experimental points on the curve.

A change in line-width occurs in the region of 220°K but the proton resonance line appears to suffer no change in the ferroelectric region. The poor experimental derivatives obtained prohibited the calculation of experimental second moments.

Figure 29 shows the results of the relaxation time measurements for the powder sample. From this curve it can be seen that $T_1$ has a value of the order of 10 sec. at 200°K which drops to approximately 0.1 sec. at 310°K. No sudden change in the slope of the curve is observed on entering or leaving the ferroelectric region.

It is usual to relate $T_1$ to a correlation time, $\tau_c$, which is characteristic of the molecular motion assisting the relaxation process (for example see reference 11). An example of such a motion could be the jumping from one potential well to another of the hydrogen atom as proposed by Mason in his theory for Rochelle Salt. If this motion is hindered by a potential barrier of height E then it is often possible to express $\tau_c$ in the form

$$\tau_c = \text{const.} \times \exp.\ (E/RT) \qquad (6.4.)$$

whence it is possible to obtain E. An approach of this type was

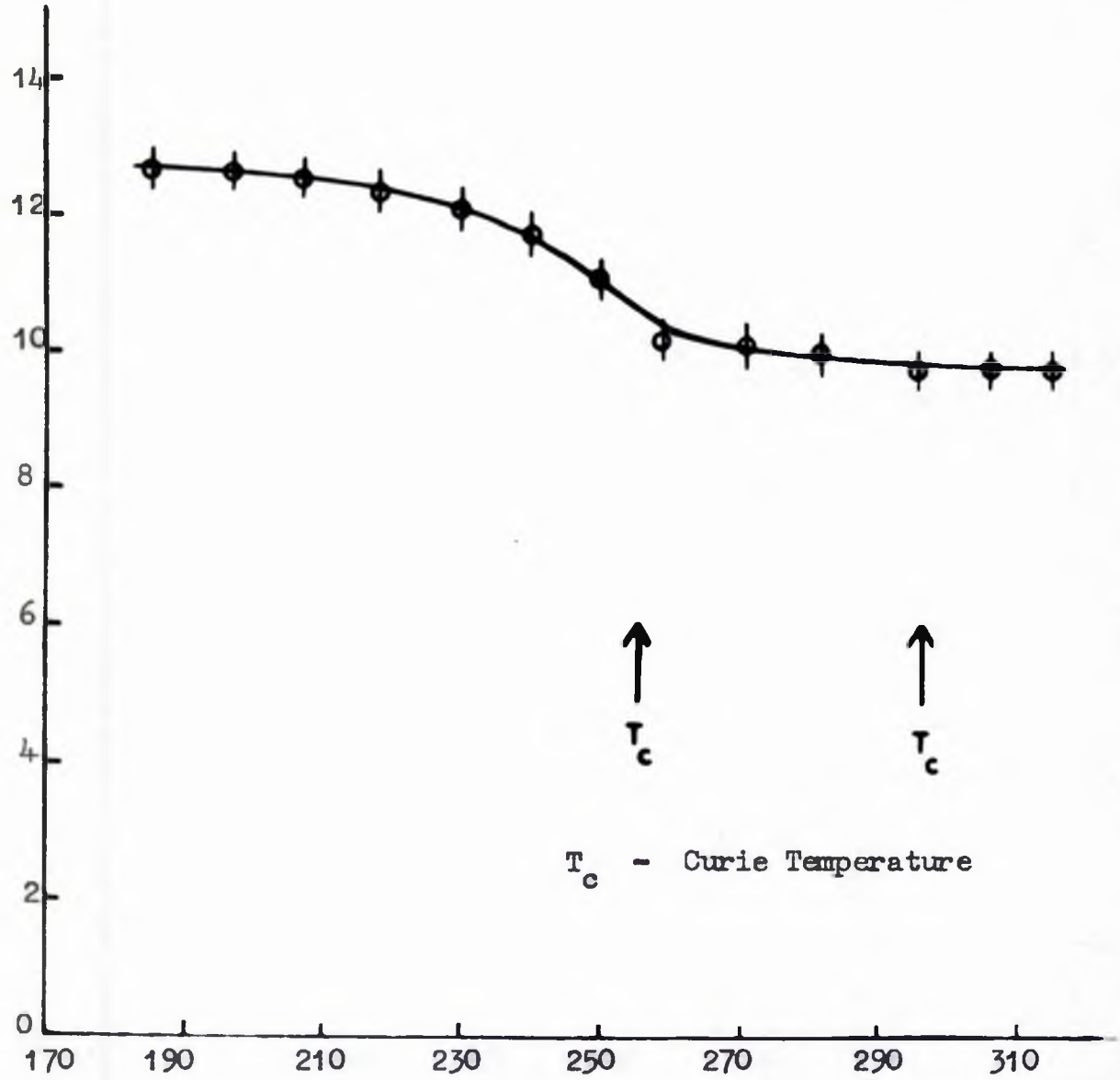
14
12
10
8
6
4
2
0
170
190
210
230
250
270
290
310
$T_c$
$T_c$
$T_c$ - Curie Temperature
Temperature °K

FIGURE 30.

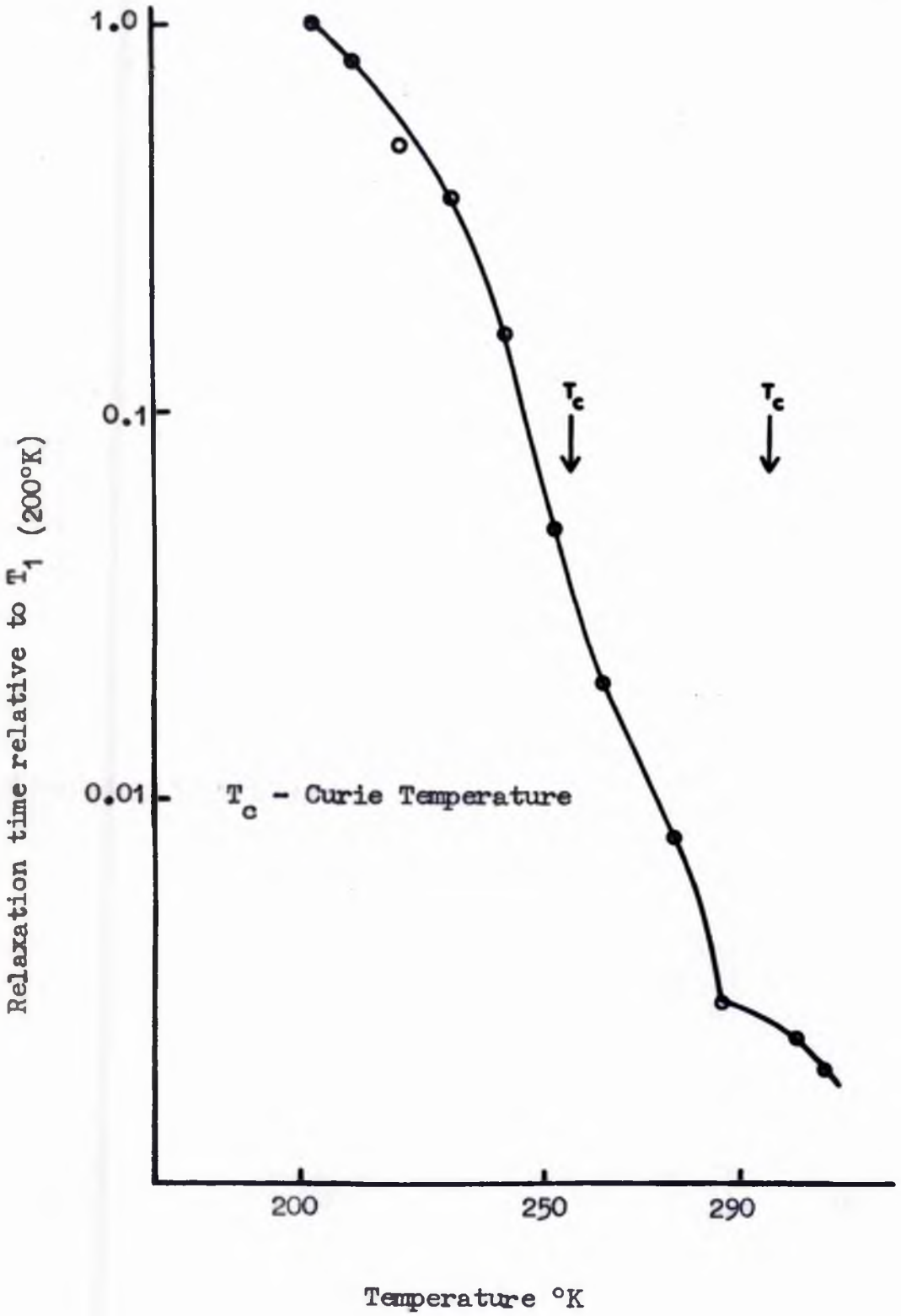
1.0
0.1
0.01
Relaxation time relative to $T_1$ (200°K)
$T_c$ - Curie Temperature
$T_c$
$T_c$
200
250
290
Temperature °K

FIGURE 31.

made but the value of E obtained was not entertained seriously as it is theoretically possible to calculate a barrier height from almost any set of relaxation time results. In addition, even if the hydrogen-bond theory were correct, it is not certain that this type of motion would play the predominant part in the relaxation process.

No great deal of information was obtained from this powder study but it did show that no anomalies occurred in either the line-width or relaxation time in traversing the ferroelectric region. Qualitatively this was thought to be rather surprising if Mason's theory is correct.

6.4.2. Single Crystal

The line-width vs. temperature curve for the single crystal of Rochelle Salt is shown in Figure 30. It is similar in character to the curve obtained from the powder sample. It shows a narrowing of the proton line in the region of 220°K but the width of the line remains constant throughout the ferroelectric range. No great change in the line shape was observed as the temperature was lowered.

As in the case of the line-width, the relaxation time data for the single crystal were very similar to the results obtained from the powder. The curve for the single crystal is shown in Figure 31. Unfortunately it was not possible to correlate $H_1$ with the signal generator voltage owing to the shape of r-f coil used. The results shown are therefore relative to the value of

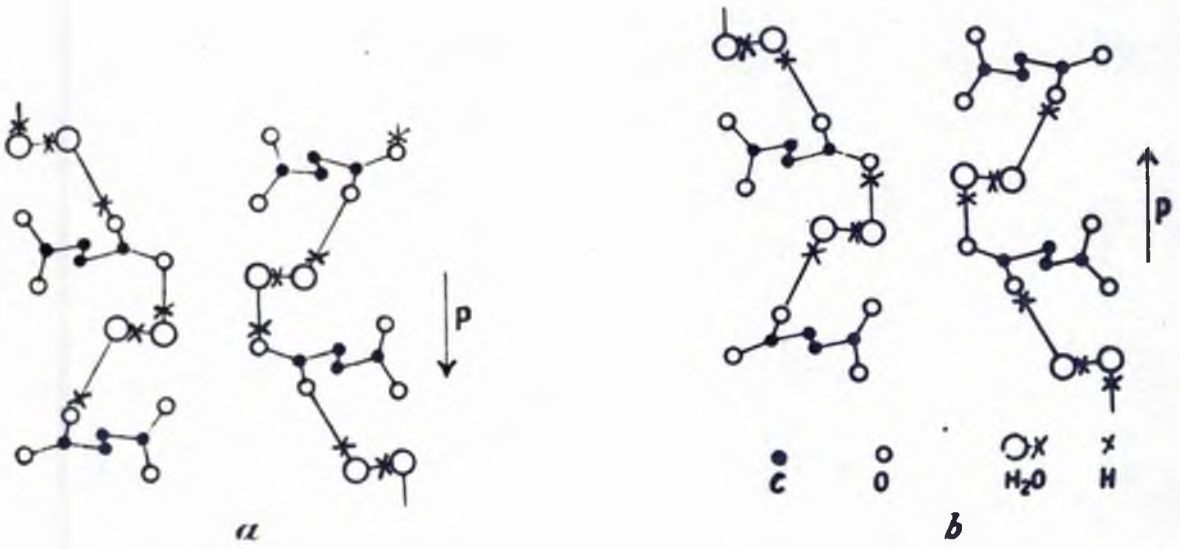


FIGURE 32.

the relaxation time at 200°K. The slope of the curve shows no discontinuities near the Curie temperatures and it is thought that the absence of any anomalous behaviour in $T_1$ or the line-width in the ferroelectric region tends to show that the hydrogen-bond theory is incorrect.

As stated previously the effect on the line-width and relaxation time of A.C. and D.C. electric fields was studied. This work was carried out at room temperature. Figure 32, taken from Wooster (60), shows a projection on the (001) plane in which tartrate and water molecules are shown but not the sodium or potassium ions. The crosses represent the assumed positions of the hydrogen atoms. It will be seen that the disposition of the hydrogen atoms leads to polarisation in the sense of the arrows P. Application of an electric field in the appropriate direction should alter the configuration from a, say, to b. This would change the orientations of the proton-proton vectors and thus a change of line-width and second moment should result. With no field present the measured values of the line-width and second moment for $H_o$ directed along the x-axis were 13.2 $\pm$ 0.3 gauss and 16.8 $\pm$ 0.5 gauss$^2$ respectively. Application of a D.C. field of 500 V/cm along the x-axis resulted in values of 13.3 $\pm$ 0.3 gauss and 17.2 $\pm$ 0.5 gauss$^2$ for the above parameters. An A.C. field of 500 V/cm at 50 c/s gave the same results. Second moments of the two configurations shown in Figure 32 were calculated according to Van Vleck's formula. In this calculation the crystal

structure as determined by Beevers and Hughes was used and the separations of the potential wells in the hydrogen-bonds were taken from Mason. It was further assumed that the second moment could be split into two parts viz.:-

1. A contribution from the hydrogen atoms other than those involved in the hydrogen-bonds. This was taken to be unaffected by the application of the electric field and was therefore not calculated as only the change in second moment was required.
2. A contribution from the hydrogen atoms which could move along the hydrogen-bonds between the two potential walls.

This calculation showed that, assuming the structure parameters to be correct, a change of about 1.5 gauss$^2$ should result in the second moment from an application of the electric field. This change is outwith the error of the experimental second moments. From this it can be deduced that either the hydrogen-bond theory is faulty or that the assumptions made in the theoretical calculation are wrong.

The electric fields produced no observable effect in the relaxation time which tends to support the belief that the hydrogen-bond theory is incorrect.

Summarising the present work on Rochelle Salt it must be emphasised that, so far, the investigations have been of an exploratory nature. Only qualitative information has been obtained, the nature of which might suggest that the hydrogen-bond theory proposed by Mason is incorrect. However, until a

great deal more work has been done in this field nothing really definite can be put forward. It is believed that research following the pattern suggested in the following section might prove fruitful in obtaining concrete information concerning the ferroelectric properties of Rochelle Salt.

6.5. Possible Programme for Future Research

Since the substitution of rubidium for potassium wipes out the ferroelectric properties of Rochelle Salt, a study of line-width and relaxation time of the proton resonance in such a substituted sample when compared with the results obtained from the normal salt should throw some further light on the hydrogen-bond theory. The magnetic environment of the protons would not change greatly and so no great change in the line-width would result. If the line-width showed this slight narrowing at 220°K and the relaxation time had the same type of variation with temperature then it would suggest that the hydrogen-bond theory was incorrect.

As stated earlier substitution of deuterium for hydrogen does not affect the properties of Rochelle Salt greatly. More information concerning the hydrogen-bond theory should thus result if deuterium were substituted in the tartrate molecules but not in the water molecules. Chemically this might prove troublesome. In addition, a study of the deuterium resonance would be interesting.

As suggested by Megaw, a movement of the potassium ions

might be the cause of the peculiar behaviour of Rochelle Salt. Therefore a nuclear magnetic resonance study of the potassium resonance should show if this motion is at all present. Since the structure of Rochelle Salt is relatively simpler with regard to potassium it should be possible to conduct this research on a more quantitative basis.

In conclusion, it can be seen that there are many interesting possibilities in this field and it is hoped to continue this work sometime in the future.

---

The author wishes to thank Professor E. R. Andrew and Dr. F. A. Rushworth for their guidance during the past three years, Professor J. F. Allen, F.R.S., for his helpful interest in this work, and Mr. J. Gerrard for the preparation of the diagrams.

# SECTION 7.

## Appendix 1.

### Estimation of $N_R$ in Urea.

Consider a unit cell of Urea.

Let the molecule lying in the (110) plane be denoted by $\alpha$ and let the molecule lying in the plane (110) be denoted by $\beta$ .

In the calculations, $( 3 \cos^2\theta_{j\ell} - 1)^2 r_{j\ell}^{-6}$ must be evaluated for all proton pairs.

Is it sufficient to do this only for protons 1 and 2 of molecule $\alpha$ or must protons 3 and 4 be treated separately along with protons 1,2,3,4 of molecule $\beta$ ?

Let proton 1 in molecule $\alpha$ have co-ords. (-A,A,C)

Consider some general proton at P, co-ords (x,y,z)

Then $$r_{P1}^2 = (x + A)^2 + (y-A)^2 + (z-C)^2$$

$$\cos \psi_{P1} = \frac{z - C}{r_{P1}} , \quad \tan \phi_{P1} = \frac{y - A}{x + A}$$ (see Fig.22)

From symmetry (assuming N-H bonds equal)

proton 4 has co-ords (A,-A,C)

and for every proton P there is a proton Q with co-ords (-x,-y,z)

$$\therefore r_{Q4} = r_{P1} , \quad \cos \psi_{Q4} = \frac{z - C}{r_{P1}} = \cos \psi_{P1}$$

$$\therefore \psi_{Q4} = \psi_{P1}$$

and $\tan \phi_{Q4} = \frac{-Y+A}{-X-A} = \frac{Y-A}{X+A} = \tan \phi_{P1}$

$$\therefore \phi_{Q4} = \phi_{P1} + \pi$$

Now from Section 5.4

$$\cos \theta_{P1} = \cos \psi_0 \cos \psi_{P1} + \sin \psi_0 \sin \psi_{P1} \cos(\phi_{P1} - \phi_0)$$

and $\cos \theta_{Q4} = \cos \psi_0 \cos \psi_{P1} + \sin \psi_0 \sin \psi_{P1} \cos(\pi + \phi_{P1} - \phi_0)$

$$= \cos \psi_0 \cos \psi_{P1} - \sin \psi_0 \sin \psi_{P1} \cos(\phi_{P1} - \phi_0)$$

$\therefore$ In general

$$\theta_{P1} \neq \theta_{Q4}$$

However, owing to symmetry it is not necessary to deal with all the neighbours of proton 4 as well as those of proton 1. Instead, having formed $\cos \psi_0 \cos \psi_{jk}$ and $\sin \psi_0 \sin \psi_{jk} \cos(\phi_{jk} - \phi_0)$ for all proton pairs including proton 1, these terms are added to obtain $\cos \theta_{P1}$ and subtracted to obtain $\cos \theta_{Q4}$ .

This also applies for protons 3 and 2.

Consider the case of proton 1 in molecule $\alpha$ with that of proton 1 (or proton 4) in molecule $\beta$ . These protons have a similar environment but it will be shown that again the $\theta$'s are not the same.

For every neighbour P of proton 1 in $\alpha$ there is an equivalent neighbour R of proton 1 in $\beta$ .

Co-ords of proton 1 in $\alpha$ are (-A,A,C)

Co-ords of proton 1 in $\beta$ are $\left(\frac{a_0}{2}-A, \frac{a_0}{2}-A, c_0-C\right)$ from crystal structure

Co-ords of P are $(x,y,z)$

Co-ords of R are $\left(\frac{a_0}{2}+x, \frac{a_0}{2}-y, c_0-z\right)$

$$\therefore r_{P1(\alpha)} = r_{P1(\beta)}$$

$$\cos\psi_{R1(\beta)} = \frac{(c_0-z)-(c_0-C)}{r_{P1(\alpha)}} = -\frac{z-C}{r_{P1(\alpha)}} = -\cos\psi_{P1(\alpha)}$$

$$\therefore \psi_{R1(\beta)} = \pi - \psi_{P1(\alpha)}$$

$$\tan\phi_{R1(\beta)} = \frac{\left(\frac{a_0}{2}-y\right)-\left(\frac{a_0}{2}-A\right)}{\left(\frac{a_0}{2}+x\right)-\left(\frac{a_0}{2}-A\right)} = \frac{A-y}{A+x} = -\tan\phi_{P1(\alpha)}$$

$$\therefore \phi_{R1(\beta)} = -\phi_{P1(\alpha)}$$

$$\therefore \cos\theta_{R1(\beta)} = \cos\psi_0\cos(\pi-\psi_{P1(\alpha)}) + \sin\psi_0\sin(\pi-\psi_{P1(\alpha)})\cos(-\phi_{P1(\alpha)}-\phi_0)$$

$$= -\cos\psi_0\cos\psi_{P1(\alpha)} + \sin\psi_0\sin\psi_{P1(\alpha)}\cos(\phi_{P1(\alpha)}+\phi_0)$$

while for proton 4 in $\beta$

$$\psi_{S4(\beta)} = \psi_{R1(\beta)} = \pi - \psi_{P1(\alpha)} \qquad \phi_{S4(\beta)} = \phi_{R1(\beta)} + \pi = \pi - \phi_{P1(\alpha)}$$

$$\therefore \cos\theta_{S4(\beta)} = -\cos\psi_0\cos\psi_{P1(\alpha)} - \sin\psi_0\sin\psi_{P1(\alpha)}\cos(\phi_{P1(\alpha)}+\phi_0)$$

Thus for every proton 1 in $\alpha$, four versions of $\theta_{jk}$ are needed to cover the cases $1(\alpha)$, $4(\alpha)$, $1(\beta)$, $4(\beta)$

i.e. $\cos\theta_{jk} =$ (1) $\cos\psi_0 \cos\psi_{jk} + \sin\psi_0 \sin\psi_{jk} \cos(\phi_{jk} - \phi_0)$

(2) $\cos\psi_0 \cos\psi_{jk} - \sin\psi_0 \sin\psi_{jk} \cos(\phi_{jk} - \phi_0)$

(3) $-\cos\psi_0 \cos\psi_{jk} + \sin\psi_0 \sin\psi_{jk} \cos(\phi_{jk} + \phi_0)$

(4) $-\cos\psi_0 \cos\psi_{jk} - \sin\psi_0 \sin\psi_{jk} \cos(\phi_{jk} + \phi_0)$

Similarly four values of $\theta_{jk}$ are required for the cases $2(\alpha)$, $3(\alpha)$, $2(\beta)$, $3(\beta)$.

Therefore, in all there are 8 typical protons to be considered in the elementary interaction unit.

## Appendix 2.

### Parameters of Trial models of Urea and 2nd Moment Results

| | $N_1H_1$ | $N_1H_2$ | $H_1\hat{N}_1H_2$ | $C\hat{N}_1H_1$ | Values of 2nd Moment $(gauss)^2$ $H_o$ along [100] | $H_o$ along [110] | $H_o$ along [001] |
|---|---|---|---|---|---|---|---|
| | 1·01 | 1·01 | 117° | 121·5° | 14·1 | 20·0 | 35·2 |
| | 1·015 | 1·015 | 119° | 120·5° | 13·7 | 19·4 | 32·8 |
| (b) | 1·02 | 1·02 | 120° | 120° | 13·9 | 19·6 | 31·8 |
| | 1·025 | 1·025 | 122° | 118° | 13·7 | 19·0 | 31·7 |
| | 1·03 | 1·03 | 123° | 117° | 13·5 | 18·5 | 31·0 |
| | 1·03 | 1·03 | 122° | 118° | 13·5 | 18·7 | 30·8 |
| | 1·03 | 1·03 | 123° | 119° | 13·2 | 19·4 | 28·5 |
| | 1·035 | 1·035 | 120° | 120° | 13·6 | 18·9 | 29·9 |
| (a) | 1·04 | 1·04 | 120° | 120° | 13·5 | 18·6 | 29·3 |
| | 1·04 | 1·04 | 119° | 121° | 13·0 | 18·6 | 28·9 |
| (c) | 1·04 | 1·04 | 122° | 120° | 12·9 | 19·2 | 27·2 |
| (d) | 1·04 | 1·04 | 120° | 118° | 13·8 | 17·8 | 31·8 |
| * | 1·04 | 0·98 | 119° | 121° | 14·1 | 20·3 | 32·7 |
| | Mean experimental values | | | | 13·6 | 18·2 | 29·0 |
| | | | | | A | B | C |

* Model proposed by Levy

## Appendix 3.

### Use of Taylor's Theorem to obtain exact agreement between assumed molecular parameters for Urea and experimental results.

Let the N-H bond be denoted by r, the $H_1N_1H_2$ bond angle by $\theta$ and the $CN_1H_1$ bond angle by $\phi$.

From Appendix 2 it can be seen that the 2nd Moment, S, is a function of the three variables $r, \theta, \phi$. Considering (a),(b),(c),(d), (Appendix 2)

by Taylor's Theorem

$$S(r, \theta, \phi) = S(r_0, \theta_0, \phi_0) + a\delta r + b\delta\theta + c\delta\phi$$

where $r_0, \theta_0, \phi_0$ refer to model (a)

and $a = \frac{\delta S}{\delta r}$, $b = \frac{\delta S}{\delta \theta}$, $c = \frac{\delta S}{\delta \phi}$

From (a) and (b)

$$a_A = -21{\cdot}0$$
$$a_B = -51{\cdot}5$$
$$a_C = -122{\cdot}5$$

from (a) and (c)

$$b_A = -0{\cdot}315$$
$$b_B = 0{\cdot}285$$
$$b_C = -1{\cdot}075$$

from (a) and (d)

$$c_A = -0{\cdot}145$$
$$c_B = 0{\cdot}400$$
$$c_C = -1{\cdot}260$$

Therefore we have

$$a_A \delta r + b_A \delta\theta + c_A \delta\phi = \delta S_A$$
$$a_B \delta r + b_B \delta\theta + c_B \delta\phi = \delta S_B$$
$$a_C \delta r + b_C \delta\theta + c_C \delta\phi = \delta S_C$$

where all a,b,c 's and $\delta$S 's are known. Hence $\delta r, \delta\theta, \delta\phi$ can be found.

The solution of the above equations is given by

$$\frac{\delta r}{\begin{vmatrix} S_A & b_A & c_A \\ S_B & b_B & c_B \\ S_C & b_C & c_C \end{vmatrix}} = \frac{\delta\theta}{\begin{vmatrix} a_A & S_A & c_A \\ a_B & S_B & c_B \\ a_C & S_C & c_C \end{vmatrix}} = \frac{\delta\phi}{\begin{vmatrix} a_A & b_A & S_A \\ a_B & b_B & S_B \\ a_C & b_C & S_C \end{vmatrix}} = \frac{1}{\begin{vmatrix} a_A & b_A & c_A \\ a_B & b_B & c_B \\ a_C & b_C & c_C \end{vmatrix}}$$

To get exact agreement with experiment

$$\delta S_A = S_A - S_{OA} = 0{\cdot}10$$
$$\delta S_B = S_B - S_{OB} = -0{\cdot}40$$
$$\delta S_C = S_C - S_{OC} = -0{\cdot}30$$

Solving for $\delta r$, $\delta\theta$, $\delta\phi$ we obtain

$$r = 0{\cdot}0062A^\circ \qquad \delta\theta = 0{\cdot}93^\circ \qquad \delta\phi = 0{\cdot}49^\circ$$

Therefore the parameters giving exact agreement with theory are

$$r = 1{\cdot}046A^\circ$$
$$\theta = 119{\cdot}1^\circ$$
$$\phi = 120{\cdot}5^\circ$$

Since the experimental accuracy is expressed as $\pm$ 0·3 gauss$^2$ we can put

$$S_A = 13{\cdot}6 \pm 0{\cdot}3 \qquad S_B = 18{\cdot}2 \pm 0{\cdot}3 \qquad S_C = 29{\cdot}0 \pm 0{\cdot}3$$

There are eight possible combinations of the allowed maximum and minimum values of $S_A$, $S_B$, $S_C$. For each combination it is possible to calculate $\delta r$, $\delta \theta$, and $\delta \phi$ and, tabulating all values of these quantities, a maximum and minimu value can be obtained for each.

A calculation of this type leads to the final values of

$$\text{N-H bond} = 1{\cdot}046 \pm 0{\cdot}01A^{\circ}$$

$$H_1N_1H_2 = 119^{\circ} \pm 2^{\circ}$$

$$CN_1H_1 = 120{\cdot}5^{\circ} \pm 2^{\circ}$$

which give a proton-proton separation in the amino group of

$$1{\cdot}80 \pm 0{\cdot}02A^{\circ}$$

## SECTION 8.

## 8. References.

1. Pake, G.E., J.Chem. Phys., 16, 27, 1948

2. Itoh, J., Kusaka, R., Yamagata, Y., Kiriyama, R., and Ibamoto, H., Physica, 19, 415, 1953

3. Gutowsky, Kistiakowsky, Pake, Purcell, J.Chem.Phys., 17, 972, 1949

4. Andrew, E.R., Bersohn, R., J.Chem.Phys., 18, 159, 1950

5. Gutowsky, H.S, Pake, G.E., J.Chem. Phys., 18, 162, 1950

6. Van Vleck, J.H., Phys. Rev., 74, 1168, 1948

7. Gutowsky, Pake, and Bersohn, J.Chem.Phys., 22, 643, 1954

8. Pake, G.E., Purcell, E.M., Phys.Rev., 74, 1184, 1948

9. Bloembergen, Purcell and Pound, Phys.Rev., 73, 679, 1948

10. Cooke, A.H., and Drain, L.E., Proc.Phys.Soc., 65, 894, 195

11. Andrew, E.R., and Eades, R.G., Proc.Roy.Doc., 218, 537, 19

12. Andrew, E.R., and Eades, R.G., Proc.Roy.Soc., 216, 398,195

13, Rushworth, F.A., Proc.Roy.Soc., 222, 526, 1954.

14. Bloch, F., Phys.Rev., 70, 460, 1946

15. Roberts, A., Rev.Sci.Instr., 18, 845, 1947

16. Hahn, E.L., Phys.Rev., 80, 580, 1950

17. Eades, R.G., Thesis, University of St Andrews, 1952

18. Rollin, B.V., Nature, 158, 669, 1946

19. Andrew, E.R., and Rushworth, F.A., Proc.Phys.Soc. B, 65, 801, 1952

20. Pake, G.E., Amer.J.Phys., 18, 47, 1950

21. Tuttle, W.N., Proc.I.R.E., 28, 23, 1940

22. Anderson, H.L., Phys.Rev., 76, 1460, 1949

23. Bloembergen, N., Nuclear Magnetic Relaxation, (Martinus Nihoff, The Hague), 1948

24. Williamson, Wireless World, April and May 1947, August 194

25. Bearden, Watts, Phys.Rev., 81, 73, 1951

26. Gutowsky, Meyer, and McClure, Rev.Sci.Instr., 24,644,1953

27. Buckley, H.E., Crystal Growth, (Wiley & Sons, Inc., New York), 1951

28. Bunn, C.W., Proc.Roy.Soc., 141, 567, 1933

29. Moore, R.W., J.Am.Chem.Soc., 41, 1060, 1919

30. Cady, W.G., Piezoelectricity, (McGraw-Hill,Inc.,New York)1

31. Mark and Weissenberg, Zeits.f.Physik, 16, 1, 1923

32. Hendricks, S.B., J.Am.Chem.Soc., 50, 2455, 1928

33. Wyckoff, R.W.G., Z.Krist., 75, 529, 1930

34. Wyckoff, R.W.G., Z.Krist., 81, 102, 1932

35. Wyckoff, R.W.G., and Corey, R.B., Z.Krist., 89, 462, 1934

36. Vaughan, P., and Donohue, J., Acta.Cryst., 5, 530, 1952

37. Kellner, L., Proc.Roy.Soc. A., 177, 456, 1941

38. Keller, W.E., J.Chem.Phys., 16, 1003, 1948

39. Waldron, R.D., and Badger, R.M., J.Chem.Phys., 18, 566, 19

40. Andrew, E.R., and Hyndman, D., Proc.Phys.Soc.,A, 66, 1187, 1953

41. Perlman, M.M., and Bloom, M., Phys.Rev., 88, 1290, 1952

42. Andrew, E.R., Phys,Rev., 91, 425, 1953

43. Herzberg, Infra-red and Raman Spectra of Polyatomic Molecules ( van Nostrand, 1945), p.439.

44. Levy and Peterson, Phys.Rev., 86, 766, 1952

45. Bersohn and Gutowsky, J.Chem.Phys., 22, 651, 1954

46. Gutowsky, Pake and Bersohn, J.Chem.Phys., 22, 643, 1954

47. Pratt and Richards, Trans.Farad.Soc., 49, 744, 1953

48. Deeley and Richards, Trans.Farad.Soc., 50, 560, 1954

49. Levy, Third International Crystallographic Congress, Paris, July 1954

50. Gutowsky, H.S., Andrew, E.R., private communication

51. Andrew, E.R., and Hyndman, D., Disc.Farad.Soc., (in press)

52. Fowler, R.H., Proc.Roy.Soc., 149, 1, 1935

53. Mueller, H., Phys.Rev., 47, 175, 1935; 57, 829,842,1940; 58, 565, 805, 1940

54. Beevers, C.A., and Hughes, W., Proc.Roy.Soc., 177, 251, 194

55. Mason, W.P., Piezoelectric Crystals, (D.Van Nostrand Compar Inc., New York), 1950

56. Ubbelohde, A.R., and Woodward, J., Proc.Roy.Soc., 185, 448, 1946

57. Mathias, B.T., and Hulm, J.K., Phys.Rev., 82, 108, 1951

58. Pepinsky, Frazer and McKeown, Phys.Rev., 94,1435,1954

59. Megaw, H.D., Acta.Cryst., 7, 187, 1954

60. W ooster, W.A., Rep. Prog. Phys., 16, 62, 1953